Provided for non-commercial research and educational use only.
Not for reproduction or distribution or commercial use.

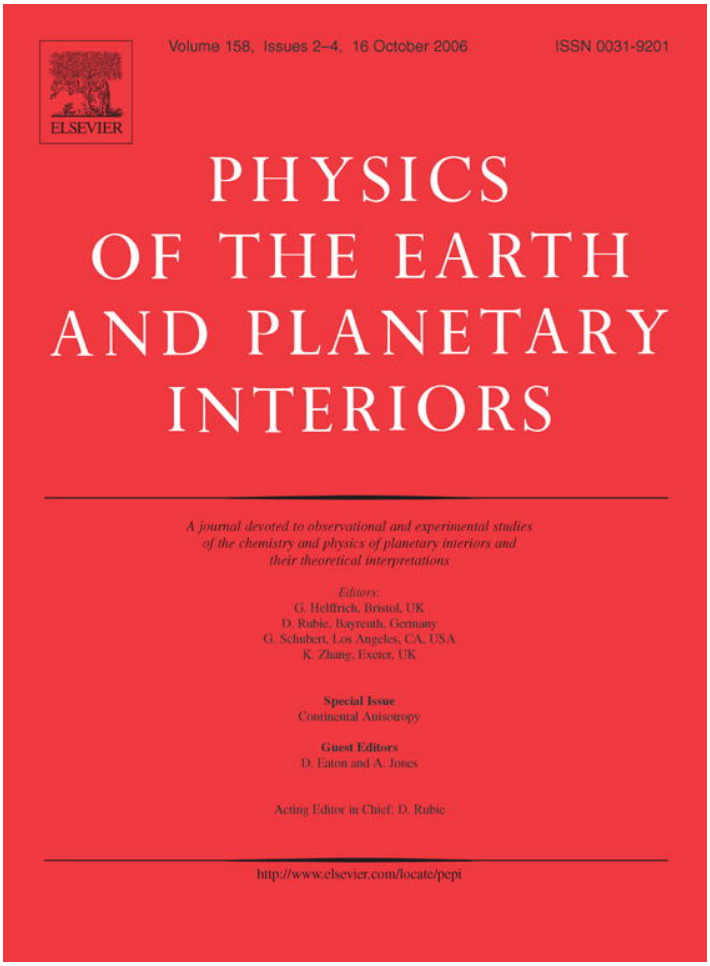

This article was originally published in a journal published by Elsevier, and the attached copy is provided by Elsevier for the author's benefit and for the benefit of the author's institution, for non-commercial research and educational use including without limitation use in instruction at your institution, sending it to specific colleagues that you know, and providing a copy to your institution's administrator.

All other uses, reproduction and distribution, including without limitation commercial reprints, selling or licensing copies or access, or posting on open internet sites, your personal or institution's website or repository, are prohibited. For exceptions, permission may be sought for such use through Elsevier's permissions site at:

http://www.elsevier.com/locate/permissionusematerial

Available online at www.sciencedirect.com
ScienceDirect
Physics of the Earth and Planetary Interiors 158 (2006) 292–320
PHYSICS OF THE EARTH AND PLANETARY INTERIORS
www.elsevier.com/locate/pepi

Seismic anisotropy beneath stable continental interiors

Matthew J. Fouch [a,*], Stéphane Rondenay [b,1]

[a] School of Earth and Space Exploration, Arizona State University, Tempe, AZ 85287, USA
[b] Department of Earth, Atmospheric and Planetary Sciences, Massachusetts Institute of Technology, Cambridge, MA 02139, USA

Received 1 September 2005; received in revised form 6 March 2006; accepted 8 March 2006

Abstract

A robust knowledge of seismic anisotropy beneath the continents is essential to our understanding of plate tectonic theory, as anisotropy provides a unique constraint on the character of past and present deformation in the lithosphere and sublithospheric mantle. This review paper summarizes the range of techniques currently available to image seismic anisotropy with passive source seismic data, and addresses current issues surrounding the observation and interpretation of continental seismic anisotropy. To this end, we present case studies for four regions where seismic anisotropy has been extensively investigated in recent years: eastern North America, the Canadian Shield, Australia, and southern Africa. Based on this full suite of results, we infer that stable continental regions generally contain seismic anisotropy that is clearly located within both the lithosphere and the sublithospheric mantle, usually to depths of at least 200 km and perhaps more. An implication of these results is that tectonic plates are, at most, only partially coupled to the underlying mantle. The results from these case studies also demonstrate that while remarkable progress in seismic anisotropy imaging has been achieved in recent years, it is clear that much more work will be required to adequately understand the origin of continental seismic anisotropy. We suggest that a more robust characterization of anisotropic parameters can only be achieved by integrating complementary seismic datasets and by incorporating constraints from key related datasets from mineral physics, magnetotellurics, gravity, and geodesy.
© 2006 Elsevier B.V. All rights reserved.

Keywords: Seismic anisotropy; Shear wave splitting; Receiver functions; Surface waves; Crust; Mantle; Plate tectonics

1. Introduction

The relationship between Earth structure at the surface and at depth is central to our understanding of the formation and evolution of Earth's interior. The matches and mismatches between observations at the surface and remotely-sensed images at depth provide critical clues regarding the nature of past geodynamic processes that shaped a region, and the current geodynamic processes that are modifying it. Two pieces of information are essential to accurately interpret these clues: the knowledge of how deformational processes alter the fabric of both the lithosphere (that is, the crust and high viscosity uppermost mantle) and the sublithospheric mantle, and the identification of when certain deformational events occurred. Because oceanic plates are relatively young (<200 Ma old) and essentially the product of conductive cooling, they generally carry only a short record of simple geologic evolution and relatively simple deformation. Continental plates, on the other hand, are much older on average and represent a complex assemblage involving a myriad of tectonic processes. Continental

* Corresponding author. Tel.: +1 480 965 9292; fax: +1 480 965 8102.
E-mail addresses: fouch@asu.edu (M.J. Fouch), rondenay@mit.edu (S. Rondenay).
[1] Tel.: +1 617 253 6299; fax: +1 617 258 6869.

0031-9201/$ – see front matter © 2006 Elsevier B.V. All rights reserved.
doi:10.1016/j.pepi.2006.03.024

Author's personal copy

interiors thus provide a unique window into past and present processes of Earth development.

One of the best ways to image deformation in Earth's interior is through the detection and interpretation of seismic anisotropy, or the dependence of seismic velocities on the direction of wave propagation and polarization. Deformation-induced fabric in the crust and mantle likely causes seismic anisotropy. The characterization of seismic anisotropy within Earth therefore provides essential clues to Earth's dynamic evolution. Over the past several decades, significant progress has been achieved to provide clearer images of seismic anisotropy, but in many cases the location of anisotropic structures has remained poorly resolved. Another significant issue is that the connections between anisotropy observations and deformational processes are still under debate. The structural origin of seismic anisotropy is therefore still not well known.

The objective of this review paper is to provide a synopsis of the ongoing debate regarding the origin and interpretation of seismic anisotropy beneath stable continental interiors, and what information it provides regarding tectonic processes on Earth. Recent advances in seismic data analysis techniques, improvements in coverage of seismic data, and related work in the mineral physics and numerical modeling communities necessitate such a review. We therefore examine a broad suite of seismic observations of continental anisotropy that have been obtained from a host of data analysis techniques. We relate these observations to tectonic processes of continental formation and evolution, paying particular attention to the connections between seismic anisotropy observations and the deformational processes inferred by them. Finally, we conclude with a discussion on the future of integrated imaging as the next essential step to improve our understanding of continental anisotropy.

1.1. Historical perspective

The effects of anisotropy on seismic wave propagation have been studied for more than a century, starting with Christoffel's 1877 theoretical treatise on seismic anisotropy, along with the notable work of Maurycy Pius Rudzki, the first recognized university professor in geophysics (Rudzki, 1897; see also Helbig and Szaraniec, 2000, and references therein). We also refer the reader to Savage (1999) and references therein for an extended history of the early development of seismic anisotropy studies. It was not until the early 1960s that a concerted effort was initiated to map lithospheric anisotropy, to understand its underlying causes, and eventually to use it as a remote sensing tool to constrain subsurface structure. Seismic anisotropy was first evaluated in detail through the incompatibility of Rayleigh and Love waves (Anderson, 1961; Aki and Kaminuma, 1963) and azimuthally varying Pn wave velocities sampling the oceanic mantle (Hess, 1964; Raitt et al., 1969). Similar azimuthal variability was later observed in surface waves sampling the oceanic (Forsyth, 1975) and continental (Crampin and King, 1977) mantle, and body waves sampling the continental lithosphere (Bamford, 1977; Hirn, 1977). With these developments, it became apparent that lithospheric/upper mantle anisotropy was a ubiquitous phenomenon, thus justifying a prominent role of radial anisotropy to 220 km depth in the global 1-D Preliminary Reference Earth Model (PREM; Dziewonski and Anderson, 1981).

The past few decades have seen the introduction of several new seismic anisotropy imaging techniques, many of which are discussed in Section 3. For instance, in the early 1980s, shear wave splitting analysis was introduced as a tool to measure in situ seismic anisotropy (Ando et al., 1980; Ando and Ishikawa, 1982; Vinnik et al., 1984; Silver and Chan, 1988). The method relies on birefringence properties of near-vertical incidence shear waves and yields superior lateral resolution of measurements of seismic anisotropy. It has been, and is still extensively used in regional studies targeting all possible tectonic environments, providing important new constraints on the evolution of their lithosphere (Silver, 1996; Savage, 1999). Other tools using teleseismic body waves to study regional anisotropy include P-wave delay times (e.g., Babuška et al., 1984), which are sensitive to dipping axes of anisotropy, and more recently receiver function methods (e.g., Bostock, 1998), which can detect sharp discontinuities in anisotropic parameters and multiple layers of anisotropic structure. Surface waves have remained a staple of seismic anisotropy imaging throughout this time (e.g., Anderson, 1961; Forsyth, 1975; Montagner and Nataf, 1986; Gee and Jordan, 1992; Forsyth and Li, 2005). Targeted, regional studies have further confirmed that anisotropy is quasi-ubiquitous in the upper mantle of all tectonic environments. It has also become clear that measurements of in situ anisotropy are fundamental to understanding lithospheric structure and evolution, and that regions displaying no apparent anisotropy are rare and therefore deserve special attention.

Until now, most of the methods described above have been used independently of one another. As we discuss at greater length in this paper, all methods have their strengths and limitations, and none has the ability to fully characterize seismic anisotropy beneath any given

Author's personal copy

target area. Accordingly, current research concentrates in part on combining the different analysis methods and using them in conjunction with independent geophysical results (e.g., Ji et al., 1996; Simons and van der Hilst, 2003; Simons et al., 2003; Audet and Mareschal, 2004) to better constrain the location of anisotropic layers and compensate for simplifying assumptions inherent to each individual technique. For a more comprehensive historical review of research in seismic anisotropy, readers are referred to Babuška and Cara (1991).

1.2. Current issues

Determining the location, magnitude, and orientation of seismic anisotropy in the crust and mantle strongly guides contemporary ideas regarding deformation and flow in the subsurface, as well as regarding interactions between boundary layers. The knowledge acquired from seismic anisotropy is thus a fundamental component in the continuing evaluation of plate tectonic theory and efforts toward imaging mantle convection. In this context, seismic anisotropy imaging addresses two fundamental goals. First, it helps identify links between crust and mantle structure, which play a key role in the interpretation of mantle deformation based on surface geology. Second, it provides a better understanding of coupling between the lithosphere and asthenosphere (or sublithospheric mantle). A key issue is that the crust/mantle interface is typically defined as a compositional boundary layer, yet in some regions is also likely a mechanical boundary layer. Conversely, the lithosphere/asthenosphere boundary is defined as a mechanical boundary layer, but is also evaluated as a compositional, thermal, and seismic boundary layer.

A key logistical challenge in imaging seismic anisotropy beneath continents is determining the lateral and depth extent of the anisotropy to address the issues mentioned above. This is challenging primarily due to geometrical constraints between sources (earthquakes) and receivers (seismometers). Theoretically, covering all areas with a dense grid of permanent stations can solve the receiver problem. In practice, however, the density of sensors in most continental regions is too sparse to adequately resolve seismic anisotropy, particularly with temporary seismic arrays where data are generally not recorded for more than ∼1–1.5 years. From a source perspective, constraining seismic anisotropy beneath continents can be particularly challenging for some methodologies, as there are inherent sampling limitations due the global distribution of seismicity.

2. What causes seismic anisotropy?

The cause of seismic anisotropy in the crust and mantle is still under significant debate. The two primary candidates are shape-preferred orientation (SPO) and lattice-preferred orientation (LPO) of Earth materials, both of which have also been invoked to explain anisotropy in the lower mantle (e.g., Lay et al., 1998; Garnero, 2000; Kendall, 2000). These anisotropic fabrics likely exist at a broad range of spatial scales, complicating imaging efforts using band-limited data (see Section 3 for further discussion on this topic). Here, we briefly summarize the properties of SPO and LPO fabrics, and their relationship to tectonic forces.

2.1. Shape-preferred orientation

Seismic anisotropy resulting from shape-preferred orientation is due to geometrical patterns of impedance contrasts that provide a preferential fast and slow direction of seismic wave propagation. In the earth, SPO in the crust can result from fluid-filled cracks due to responses to stress (e.g., Crampin et al., 1984), while SPO in the mantle may be generated by melt-filled cracks or lenses, or compositional lamellae (e.g., Kendall, 1994, 2000; Zimmerman et al., 1999; Braun et al., 2000; Walker et al., 2004). The fast polarization direction from SPO occurs along the long axis or plane of structures such as tubules or lenses since, based upon Fermat's Principle, finite-frequency seismic wavefronts will preferentially propagate along faster velocity material. The degree of anisotropy is proportional to the magnitude of velocity contrasts and the relative volumes of fast and slow material in the matrix.

SPO is thought to be a significant cause of seismic anisotropy beneath mid-ocean ridges and perhaps some portions of subduction systems. Similarly, continental rift zones contain a range of evidence suggesting that SPO due to decompression melting plays an important role in the development of seismic anisotropy. Beneath stable continental interiors with thick lithospheres, however, SPO is usually perceived as a local crustal phenomenon with less broad-scale influence on most seismic anisotropy observations.

2.2. Lattice-preferred orientation

It is generally believed that a key cause of seismic anisotropy in the crust and mantle is the lattice-preferred orientation of crystallographic axes of elastically anisotropic minerals. Biotite and hornblende are primary candidates for crustal anisotropy (Mainprice

Author's personal copy

and Nicolas, 1989; Babuška and Cara, 1991). In the upper crust, materials exhibiting foliation and LPO have likely undergone deformation at depth in the mid- or lower-crust followed by partial or full exhumation. Globally generalizing the location and geometry of middle and lower crustal anisotropy, however, is more challenging due to a range of varying results from seismic reflection profiles (Meissner et al., 2002). In the upper mantle, olivine is assumed to play a dominant role in the generation of seismic anisotropy (e.g., Karato, 1987; Nicolas and Christensen, 1987; Karato and Wu, 1993; Mainprice and Silver, 1993; Ben-Ismaïl and Mainprice, 1998; Holtzman et al., 2003), although a recent petrophysical study indicates that orthopyroxene may also have a significant impact (Ben-Ismaïl et al., 2001). A more appropriate term for LPO might be crystallographic preferred orientation (CPO) (Holtzman et al., 2003), but since the literature historically refers to this fabric as LPO we will follow this convention. While the maximum depth of upper mantle anisotropy is still under debate, olivine likely deforms in the dislocation creep regime (the deformation regime in which LPO can develop) to depths of 200–400 km (e.g., Karato and Wu, 1993; Podolefsky et al., 2004). We note, however, that the effect of pressure on mineralogy likely plays an important role on anisotropy, as the slip system of olivine may change significantly at depths >250 km in the upper mantle (Couvy et al., 2004; Mainprice et al., 2005). Additionally, there is growing evidence for the existence of anisotropy in the mantle transition zone and the uppermost lower mantle (e.g., Fouch and Fischer, 1996; Montagner and Kennett, 1996; Trampert and van Heijst, 2002; Chen and Brudzinski, 2003; Beghein and Trampert, 2004b; Wookey and Kendall, 2004; Tommasi et al., 2004a).

Theoretical finite strain models suggest that under relatively dry conditions, olivine *a*-axis (the seismically fast direction) align roughly parallel to the direction of maximum finite extension (e.g., McKenzie, 1979; Ribe, 1989, 1992; Ribe and Yu, 1991; Wenk et al., 1991; Blackman et al., 1996; Tommasi, 1998; Wenk and Tomé, 1999; Kaminski and Ribe, 2001). Experimental data corroborate this result for uniaxial deformation (Karato, 1987; Nicolas and Christensen, 1987), although shear experiments indicate that at large strains, olivine *a*-axis orientation is controlled by the flow direction (Zhang and Karato, 1995; Zhang et al., 2000). Experimental results have also shown that water plays a critical role in modifying mantle velocities and LPO development (Karato and Jung, 1998; Jung and Karato, 2001; Katayama et al., 2004, 2005). These effects significantly modify predictions of shear wave splitting where adjacent wet and dry regions may exist (Lassak et al., 2006). Similarly, Holtzman et al. (2003) have shown that the presence of melt can drastically modify LPO behavior. They found that melt generation will typically weaken LPO fabric, but further strain partitioning will reorient olivine *a*-axis to be orthogonal to the primary shear or flow direction. Field samples (e.g., Ben-Ismaïl and Mainprice, 1998; Mehl et al., 2003) also provide additional constraints on inherent mantle fabric that, to first order, are similar to laboratory results with respect to strength and orientation of anisotropy, and yield evidence for the broad range of potential effects to the development of LPO described above.

2.3. Relationship of tectonic forces to crust and mantle fabric

While SPO and LPO develop in both the crust and mantle due to tectonic forces, they may manifest themselves in very different ways for the same stress geometry, yielding conflicting anisotropic signals. For instance, crustal SPO could develop from cracks with a long axis (and therefore fast polarization orientation) orthogonal to the direction of maximum extension. Conversely, LPO in the mantle (assuming, for a moment, olivine deforming under relatively dry conditions) would develop parallel to the same extension direction and would thereby produce a fast polarization orientation parallel to the extension direction. In many cases, these opposing structures would yield a complex or undecipherable anisotropic signal, yet the coupling between crust and mantle structure remains rather simple. This issue must be kept in mind when interpreting results from currently available methodologies as well as during the development of new analysis techniques.

3. Methods

This section contains a summary of the methods currently used for imaging continental seismic anisotropy. We provide an overview of the theoretical foundations and implementation of each technique, followed by a discussion of their strengths and weaknesses. Fig. 1 shows a synopsis of the relative sampling areas for each type of dataset.

3.1. Shear wave splitting

Arguably the most well-studied and particularly direct manifestation of seismic anisotropy is shear wave splitting, in which a shear wave propagates through an anisotropic medium and splits into two quasi-shear

Author's personal copy

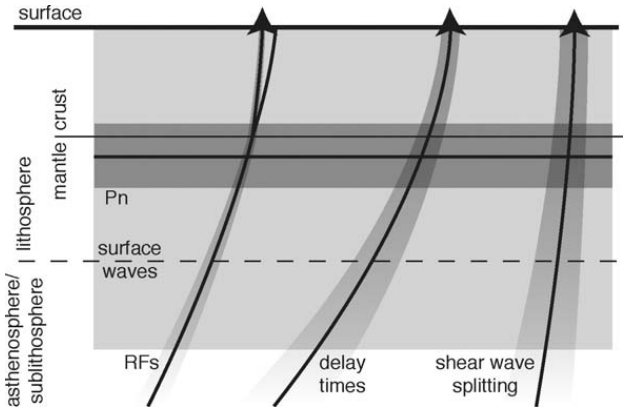

Fig. 1. Schematic raypaths and sampling regions for the seismic analyses described in this study, including Pn, Ps receiver functions (RFs), body wave delay times, body wave shear wave splitting, and surface waves. Shaded areas represent sampling areas including relative Fresnel zone volumes but are not to scale. Pn and surface waves sample lateral structure and therefore have better depth resolution, while body waves sample predominately vertical structure and therefore have better lateral resolution.

waves with orthogonal polarizations that propagate at different velocities. In an anisotropic medium with a horizontal symmetry axis, near-vertically traveling shear phases split into fast and slow components with orthogonal polarization directions. The splitting parameters are the polarization of the fast split shear wave ϕ, and the travel time difference between the fast and slow split shear waves δt. Values of ϕ and δt represent the path-integrated effects of anisotropy on the shear wave and are highly dependent upon the simplicity (i.e., single-layer anisotropy) or complexity (i.e., dipping layers or multiple zones of anisotropy) of the geometry of the anisotropic material.

Analysis of shear wave splitting on local and teleseismic shear waves has evolved into a very commonly used tool for constraining continental seismic anisotropy (e.g., Kind et al., 1985; Silver and Chan, 1988; Vinnik et al., 1989, 1992; Savage et al., 1990; Gao et al., 1997; Levin et al., 1999; Fouch et al., 2000; Park and Levin, 2002) (see http://geophysics.asu.edu/anisotropy/upper for a comprehensive list of published shear wave splitting studies using core phases). Methods of shear wave splitting analysis can be divided into general groups, where the search for the optimal pair of splitting parameters is based on: (1) the minimization of a penalty function which represents the difference between observed and predicted transverse components (e.g., Vinnik et al., 1989); (2) the maximization of the cross-correlation between the fast and slow components or linear particle motion (e.g., Bowman and Ando, 1987; Iidaka and Niu, 1998; Levin et al., 1999); (3) the minimization of the ratio of covariance matrix eigenvectors; and (4) the minimization of energy on the corrected transverse component reassembled from the optimal fast and slow components (e.g., Silver and Chan, 1988, 1991). We note that this last method can be applied to P-to-S (Ps) converted waves where transverse energy results primarily from seismic anisotropy (see Section 3.2 for further discussion).

Many variations on these basic methodologies have been developed. For instance, the widely used multi-event approach of Wolfe and Silver (1998) utilizes methods 3 and 4 by summing misfit surfaces of splitting analyses from different events recorded at a given station. This technique effectively averages out splitting signal variation, and provides the best model parameters for a single-layer anisotropy model with a horizontal fast axis. Another recently developed method is the cross convolution algorithm by Menke and Levin (2003), which is designed to minimize the misfit between a given anisotropic earth model and observed waveform data.

Several techniques utilize backazimuthal variations in shear wave splitting parameters to detect the effects of dipping or multiple layers of anisotropy. For instance, Chevrot (2000) considers backazimuthal variations in transverse energy of core phases to obtain a single set of best-fitting splitting parameters for a seismic station. This method provides an estimate of the splitting intensity that provides an additional measure of the scales of anisotropy, but requires a broad range of backazimuthal coverage. Other analysis methods have been published to evaluate more complex anisotropic structures, such as a single anisotropic layer with a dipping fast axis or multiple anisotropic layers (e.g., Savage and Silver, 1993; Özalaybey and Savage, 1995; Hartog and Schwartz, 2000; Davis, 2003; Menke and Levin, 2003; Schulte-Pelkum and Blackman, 2003; Walker et al., 2004; Eberhart-Phillips and Henderson, 2004). For instance, Hartog and Schwartz (2000) and Walker et al. (2004) use similar approaches where they solve the Christoffel equation to predict splitting parameters. They then perform a grid search to find the optimum orientation (including fast axis azimuth and dip) of the tensor that minimizes the difference between the trial and observed splitting parameters. This type of analysis is easily extended to examine multiple layers of anisotropy. Finally, we note that Teanby et al. (2004) have recently introduced an automated shear wave splitting analysis tool. With this tool, shear wave splitting is evaluated for a range of waveform window lengths, and the stability of the measurement is evaluated using cluster analysis and a final data window is selected based on the lowest cluster error. Fast polarization orientation and splitting time estimates are therefore objective and internally consistent.

Author's personal copy

Shear wave splitting analyses possess a number of very appealing attributes. First, the standard methodologies typically used are relatively simple and computationally inexpensive, which likely explains its popularity since its introduction in the 1980s and thus the rich database of thousands of measurements currently available. In a related vein, an important constraint provided by shear wave splitting analysis is the formal estimation of measurement error, which is critical to the interpretation of similarities and differences in datasets, as well as comparisons of datasets using different methodologies. Second, lateral resolution of structure is generally good and provides important constraints on broad-scale fabric. Lateral resolution is determined by the Fresnel zone of the phase. As an example, an SKS phase with a 12 s dominant period possesses a Fresnel zone that is 90 km in radius at 150 km depth, assuming a Fresnel zone approximation using the half-wavelength criteria for a vertically incident ray. However, shear wave splitting possesses sensitivity to smaller-scale structures that can also be detected for tightly spaced arrays (e.g., Rümpker and Ryberg, 2000; Favier and Chevrot, 2003; Chevrot et al., 2004; Fouch et al., 2004b). In the presence of very small-scale anisotropic variations, however, frequency-dependent shear wave splitting effects must be evaluated (e.g., Gledhill, 1993; Marson-Pidgeon and Savage, 1997; Fouch and Fischer, 1998; Rümpker and Ryberg, 2000; Favier and Chevrot, 2003; Fouch et al., 2004b). Finally, given adequate backazimuthal and incidence angle coverage, shear wave splitting provides an opportunity to extract structural complexity (i.e., dipping or multiple anisotropic layers) from the anisotropic signal.

Despite (or perhaps in part due to) the popularity of shear wave splitting analyses, the approach has its limitations. First, the number of published shear wave splitting studies now exceeds 100 publications, leading to a broad range of results from very different methodologies with varying levels of quality control. A related problem is that splitting parameters for core phases such as SKS and SKKS using the same source–receiver pair are not always compatible with one another (James and Assumpçao, 1996; Özalaybey and Chen, 1999; Niu and Perez, 2004), suggesting that the extraction of shear wave splitting parameters is not always as simple as assumed. Second, shear wave splitting analyses using core phases do not provide any constraint on the depth location of the anisotropy, since the splitting could originate in the lowermost mantle (e.g., Lay et al., 1998; Kendall, 2000), the uppermost lower mantle (Wookey et al., 2002; Wookey and Kendall, 2004), or scatterers in the crust and/or mantle (Hedlin and Shearer, 2000). Third, methods of error estimation vary, limiting a complete comparison of shear wave splitting studies in many cases. The overall result is a heterogeneous compilation of shear wave splitting analyses that, in many cases, cannot be directly compared both internally among various splitting studies and externally with other observations of seismic anisotropy. Finally, to provide adequate constraints for complex anisotropic structure that is identifiable only via backazimuthal variations, we estimate that an average station must record for periods >1–1.5 years to attain a sufficient data coverage. As with many of the methods described here, we note that obtaining robust backazimuthal observations is never possible if the station is poorly located relative to world seismicity (e.g., Wysession, 1996; Chevrot, 2000).

3.2. Receiver functions (RFs)

The receiver function technique has been used for 30 years to investigate discontinuities in material properties of the subsurface, mostly in the crust, upper mantle and mantle transition zone (e.g., Vinnik, 1977). This approach relies primarily on the identification of P-to-S-wave conversions (Ps) which occur at sharp discontinuities and appear as secondary pulses in the coda of local or teleseismic P-waves. Since single Ps phases generally rise just above the noise level of seismic recordings, traces from several events are usually stacked to increase their signal to noise ratio. This operation requires source-normalization and proper moveout correction (i.e., delay-time versus incidence angle) of the traces. For source-normalization, the vertical component of each event recording is used as an estimate of that event's source-time function. It is then deconvolved from the radial and transverse components (which contain most of the Ps signal) to obtain an estimate of the ground's impulse response. The result of this process is called the RF. The moveout correction is calculated by assuming that the background velocity model is known and that discontinuities are planar and generally horizontal. The stacked receiver functions are a map of 1-D structure below the seismic station, where the Ps phase delay indicates the depth of discontinuities, and the amplitude of Ps represents the strength of the impedance contrast.

Basic seismic theory indicates that Ps signal generated and traveling in a 1-D (horizontally layered) isotropic medium is entirely contained in the plane formed by the vertical and radial components of the seismogram (i.e., the sagittal plane). Any added complexity, such as dipping layers, anisotropy, or more generally 3-D scattering will produce Ps signal observable on both radial and transverse components. Although

Author's personal copy

most RF studies assume 1-D isotropic background media (e.g., Ammon et al., 1990; Dueker and Sheehan, 1997), recent efforts have exploited radial and transverse Ps waveforms to detect and characterize anisotropic media. These analyses rely on RF sections displaying variations in Ps amplitude and polarity as a function of event's back-azimuth and epicentral distance.

Three different techniques have been proposed to recover anisotropic parameters from receiver functions: (1) *forward RF modeling*, where RF sections are generated using reflectivity or ray theoretical synthetics, and where anisotropic parameters are adjusted manually to recreate the observed data (e.g., Bostock, 1998; Savage, 1998; Frederiksen and Bostock, 2000; Park et al., 2004); (2) *Monte Carlo approaches*, where RF sections are generated as in the first technique, but where the parameter space is more thoroughly explored through directed search algorithms (e.g., Levin and Park, 1997; Frederiksen et al., 2003); and (3) *1-D Born scattering inversion*, where RFs are inverted for anisotropic property perturbations at depth (Bostock, 2003; Bank and Bostock, 2003). The first two techniques generally assume hexagonal or orthorhombic symmetries, and recover the azimuth and dip of the principal axis of anisotropy. The methodology of Frederiksen et al. (2003) is more general as it helps mitigate the tradeoff between anisotropy and layer dip. The third technique inverts for 1-D (horizontally layered) perturbations to the most general form of anisotropy, involving 21 independent terms of the elastic tensor plus density.

Receiver function analyses of anisotropic parameters possess several desirable attributes. First, they yield the best vertical resolution of all the techniques discussed in this section, allowing for the detection of sharp vertical variations in anisotropy and multi-layered anisotropy, and the determination of the depth extent of anisotropic layers. The vertical resolution is controlled by the wavelength of the Ps phase, λ, which depends on the spectral content of the recorded signal and the velocity of the medium. Material property gradients occurring over a depth range of $\sim<\lambda/2$ (average S wavelengths are 3.5 and 4.5 km in the crust and upper mantle, respectively, for a 1.0 s dominant period) can be identified and well characterized. This quantity also corresponds to the minimum thickness resolvable for discreet homogeneous layers. Second, RF techniques afford appreciable resolution of lateral variations in anisotropic parameters. Lateral resolution is determined by the Fresnel zone of the Ps wave, allowing for the detection of changes occurring over <25 km and 45 km for the lower crust and lithosphere (~150 km), respectively.

The main limitations of RF techniques are related to the non-linearity and underdeterminedness of the problem. Non-linearity is due to coupling between the background medium and the material property perturbations that are inverted for, as in the method of Bostock (2003). The problem may be linearized by assuming that the perturbations are small (i.e., <5%) relative to the background medium. Underdeterminedness affects all the RF techniques, as the number of parameters describing anisotropic material property perturbations (22 parameters) and their location (3 parameters) is always greater than the number of data points. The underdetermined problem is solved by simplifying the parameter search space, i.e., assuming simple symmetries (e.g., hexagonal) and limiting the number of layers. Assumptions that are adopted to accommodate for non-linearity and underdeterminedness are not always valid and can therefore cause significant errors in parameter estimation.

3.3. Relative arrival/delay times

The analysis of variations in relative travel times of body waves is a less extensively used, but important, diagnostic that provides valuable additional constraints on the strength and orientation of seismic anisotropy. This approach consists of measuring relative delay times of regional and/or teleseismic waves (generally P, but also S) that illuminate single stations from different azimuths (e.g., Babuška and Cara, 1991, and references therein). Relative delay times are obtained by calculating the difference between the actual arrival times of a given phase and that predicted for a reference background medium. The mean difference is then set to zero. Resulting values are generally mapped stereographically to display variations as a function of azimuth and incidence angle of the incoming rays. Negative and positive delay times indicate fast and slow orientations, respectively, and may be associated with the orientation of principal axes of anisotropy. For typical teleseismic distance ranges, P-waves have incidence angles that vary between 50° and 0° (vertical), and can therefore help characterize dipping axes of anisotropy. Results are analyzed either graphically, by visually identifying principal directions and making inferences about regional anisotropy (e.g., Babuška et al., 1984), or analytically, by inverting the relative delay-time data for anisotropic parameters of the subsurface (e.g., Bökelmann, 2002). In either case, particular attention is paid to regional patterns that cannot be explained by lateral velocity heterogeneities and therefore require the presence of anisotropy. We also note

Author's personal copy

that relative delay times are occasionally used in concert with shear wave splitting results to provide constraints beyond those available with shear wave splitting alone (e.g., Buchbinder, 1989; Levin et al., 1996; Guilbert et al., 1996; Bökelmann, 2000; Fouch et al., 2004b; Schmid et al., 2002).

The analysis of relative delay times possesses three main positive attributes. First, the basic delay time calculation is very simple and rapid to compute, providing an immediate first-order assessment of anisotropic trends in the upper mantle. Second, by virtue of P-wave ray geometry, relative delay times of these waves yield constraints on dipping axes of anisotropy. This is a feature that is considerably more difficult to identify in other approaches. Third, the method of delay times offers good resolution to lateral variations in anisotropic parameters. The resolution is once again controlled by the Fresnel zone which, at lithospheric depths, has a diameter of ~50–100 km.

The main limitation of relative delay time analysis is the tradeoff between anisotropy and lateral velocity heterogeneity. Local and regional variations in isotropic velocities can produce values of azimuthally varying delay times similar to those caused by anisotropy. It is clear that this issue cannot be resolved unless both types of anomalies are modeled simultaneously. This can be achieved by inverting travel-time delays for anisotropic velocity perturbations. However, such generalization increases the problem's underdeterminedness, and therefore requires the integration of other independent datasets (see Section 5.2). A second noteworthy limitation of the method is its stringent data coverage requirement. To clearly identify potential axes of anisotropy, a station must be illuminated from all azimuths and with a comprehensive range of epicentral distances. These two conditions may not be met if the station is poorly located relative to world seismicity (e.g., Wysession, 1996; Chevrot, 2000) or if the recording period is not long enough. Using the same approach as for SKS splitting analysis, we estimate that an average station must record for periods >1–1.5 years to attain a sufficient data coverage for undertaking meaningful relative delay time analyses.

3.4. Pn anisotropy

The Pn phase is a head wave that propagates along (or just beneath) the crust–mantle boundary (Moho) at uppermost mantle velocities. First utilized by Hess (1964) in one of the cornerstones of modern seismic anisotropy studies, azimuthal variations in Pn arrival times were used to infer lateral variations in seismic anisotropy beneath ocean basins. Information obtained from this type of analysis is a P-wave fast polarization direction and an anisotropic magnitude. We note that the exploration seismology community has also extensively utilized refracted P-wave anisotropy in shallow crustal imaging; however, in the current work, we focus on applications that enable imaging of structure via natural sources.

Arrival times of Pn phases are obtained from a variety of sources, including the ISC catalog (e.g., Smith and Ekström, 1999), and hand-measured arrival times (e.g., Hearn, 1996). In Hearn's approach, Pn arrival times from a single source at multiple receivers are used to construct a travel time curve, where the slope of the best-fitting line gives an estimate of the Pn velocity for the suite of source–receiver paths. Azimuthal and velocity information are then combined for each path and inverted for models of anisotropic magnitude and fast polarization direction assuming a horizontal symmetry axis. Conversely, in the Smith and Ekström approach, ISC arrival times are employed to obtain two-station Pn differential times, which are then used to determine Pn velocities along a given path. Following the removal of significant outliers, raypaths are assigned velocities and cap-averaged with caps of 1.5° and 3°. Individual tectonic regions are then evaluated for seismic anisotropy by determining the model that best fits the velocity and azimuth dataset.

The advantage of Pn anisotropy analysis is that it provides a direct estimate of seismic anisotropy in the uppermost mantle, with limited uncertainty as to the depth location of the layers surveyed. Although studies are limited in number and global coverage at present, current regional coverage is good enough to provide important constraints for some parts of Earth otherwise nearly unsampled from a seismic anisotropy perspective. Regions of extensive shallow seismicity are ideal locations for this type of analysis and are currently underexploited.

Limitations to Pn anisotropy analysis include the standard tradeoff between apparent anisotropy due to seismic velocity heterogeneity and anisotropy due to aligned fabric. Observations of Pn anisotropy also cannot provide constraints on depth variations of anisotropy, since Pn waves only sample velocities near the Moho. In addition, lateral resolution may suffer from the lack of adequate source–receiver path distribution often encountered in current experimental settings. In a similar vein, Pn raypaths do not provide enough information to assume anything but horizontally oriented anisotropy, which eliminates the evaluation of complex geometries of anisotropy.

Author's personal copy

3.5. Surface waves

While body waves provide a direct measure of mantle anisotropy with good lateral but poor depth resolution, the opposite is true for surface wave models. Surface (Rayleigh and Love) waves propagate horizontally in the earth's crust and upper mantle from a source to a receiver and are therefore sensitive to primarily shear wave structure at depths of ~1/3 of a given wavelength. Surface wave analyses can therefore provide important constraints on seismic anisotropy that are independent from those obtained with the body wave techniques described above.

Two types of anisotropy, radial (vertical) and azimuthal (horizontal), are normally evaluated. The existence of radial anisotropy in the upper mantle has been well established from the discrepancy of Love and Rayleigh wave propagation, while the existence of azimuthal anisotropy is usually determined by changes in Rayleigh wave propagation with direction. Models of surface wave anisotropy are determined by a broad range of techniques (e.g., Anderson, 1961; Forsyth, 1975; Dziewonski and Anderson, 1981; Kawasaki and Kon, 1984; Tanimoto and Anderson, 1985; Montagner and Nataf, 1986; Gee and Jordan, 1992; Gaherty and Jordan, 1995; Laske and Masters, 1998; Ekström, 2001; Trampert and Woodhouse, 2001; Boschi and Ekström, 2002; Shapiro and Ritzwoller, 2002; Gung et al., 2003; Beghein and Trampert, 2004a; Smith et al., 2004; Forsyth and Li, 2005). However, nearly all datasets are first determined by measuring surface wave dispersion curves that determine the maximum sensitivity to velocity structure at depth as a function of frequency. These frequency-dependent dispersion measurements (in terms of phase or group velocities) are then used in various forms of inversions to determine the 1-, 2-, or 3-D velocity and anisotropy structure of a region. Inversion approaches include standard least-squares type methods, as well as more robust methods such as the Monte Carlo-type Neighborhood Algorithm (e.g., Sambridge, 1999a,b). A slight twist on these techniques is the two-plane-wave inversion approach (Li et al., 2003; Forsyth and Li, 2005), which accounts for the effects of structure located outside of a given study area by representing an incoming wavefield as the interference of two plane waves with different amplitudes, phases, and propagation directions. We also note that fully 3-D models of anisotropy that examine both radial and azimuthal structure have been recently developed (e.g., Montagner and Guillot, 2000; Montagner, 2002).

A primary advantage of surface wave analyses is that they provide better depth constraints on seismic anisotropy than shear wave splitting at depths down to ~300 km. New methods that combine body and surface wave data, and benefit from denser datasets afforded by portable seismic arrays, have a lateral resolution of <100 km. Surface wave analyses also provide a good bridge between body wave and normal mode analyses because they provide both good depth resolution as well as long-wavelength lateral resolution.

The major limitation of surface wave inversions for anisotropy is that the first-order phase velocity signal can be explained either by lateral variations in isotropic properties or anisotropic parameters. Choices of inversion parameters, such as regularization values, also have an important effect on modeled anisotropic structure. Assessment of velocity/anisotropy tradeoffs is therefore required in this process. In addition, sensitivity of surface waves to structure deeper than ~300 km is challenging and only possible with a few datasets including higher modes. Given these and other resolution issues, it is also desirable to complement large-scale surface wave models of anisotropy with a comprehensive set of body wave observations.

4. Structural origins of continental seismic anisotropy: case studies

End-member hypotheses have been proposed to explain shear wave splitting patterns in continental settings. First, many continental regions exhibit splitting patterns that appear closely related to surficial geologic features, suggesting that seismic anisotropy exists primarily in the lithosphere and is related to fabric that was generated by the most recent significant tectonic event (e.g., Silver, 1996; Barruol et al., 1997) or that lithospheric and sublithospheric deformation are coherent. Conversely, some regions exhibit patterns of seismic anisotropy more closely related to the local direction of absolute plate motion (APM) in the hotspot reference frame (e.g., Vinnik et al., 1989, 1992), suggesting that seismic anisotropy exists primarily in the sublithospheric mantle and is generated by fabric resulting from mantle flow. A twist on this end-member model is that mantle may flow both beneath and around continental keels with complex morphologies, generating a fabric that mimics the keel shape. More recently, a number of seismic anisotropy observations have led to the conclusion that a combination of both lithospheric and sublithospheric fabric is responsible for the seismic anisotropy observations (e.g., Levin et al., 1999; Fouch et al., 2000; Becker et al., 2003; Gung et al., 2003; Behn et al., 2004; Walker et al., 2004).

Author's personal copy

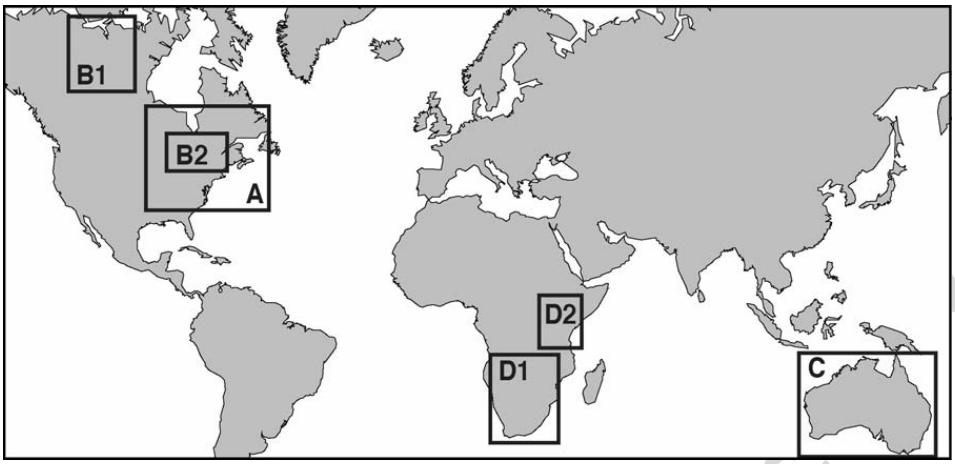

Fig. 2. Regions of case studies examined in this study including eastern North America (box A), subregions of the Canadian Shield (boxes B1 and B2), Australia (box C), and southern Africa (boxes D1 and D2).

In light of this current debate, we review several regional case studies of continental seismic anisotropy (Figs. 2–7). We focus on the stable continental settings of eastern North America, the Canadian Shield, Australia, and southern Africa based chiefly on the number of seismic anisotropy studies performed in each of these areas. We emphasize that in many cases these studies were published several years apart and therefore have not yet been addressed in the common framework we seek here.

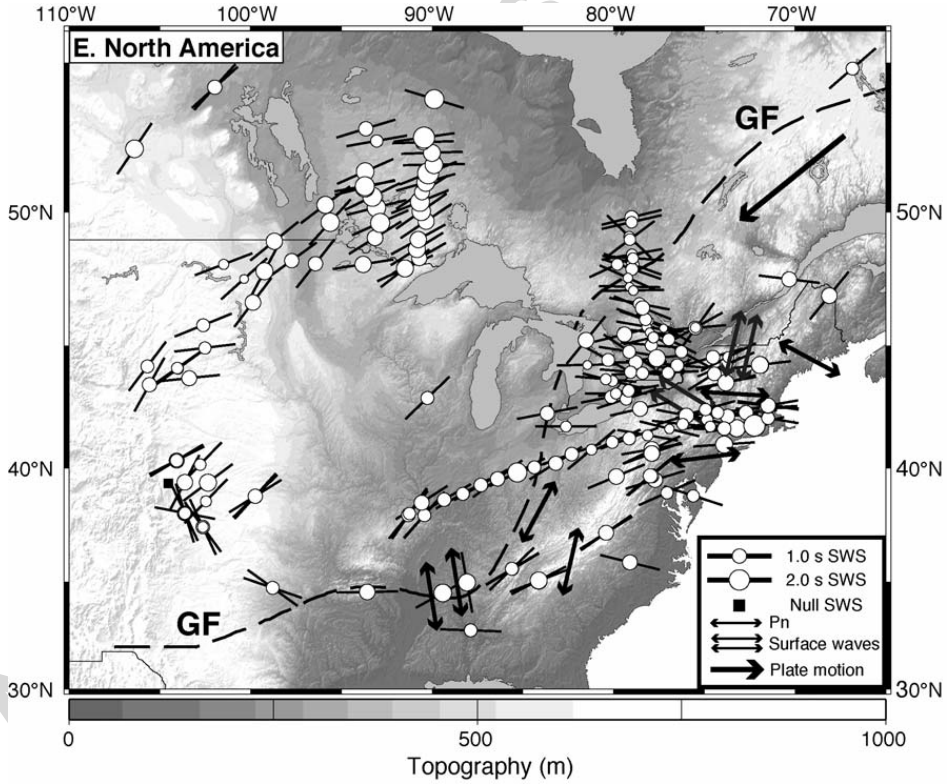

Fig. 3. Summary of published azimuthal anisotropy results for eastern North America. See text for list of individual studies represented in this figure. Dashed line denotes surface boundary of Grenville Front (GF). Shear wave splitting fast polarization directions are denoted by single black bars; open circles are scaled to splitting time values; null shear wave splitting measurements are shown by black boxes. Pn fast polarization direction is denoted by single small black arrow; surface wave fast directions shown by double black arrow. Large black arrow denotes absolute plate motion direction (Gripp and Gordon, 2002). In this region, seismic anisotropy appears to be controlled by a combination of lithospheric fabric and sublithospheric fabric generated by flow around and beneath the regional lithospheric keel as defined by the regional surface wave images.

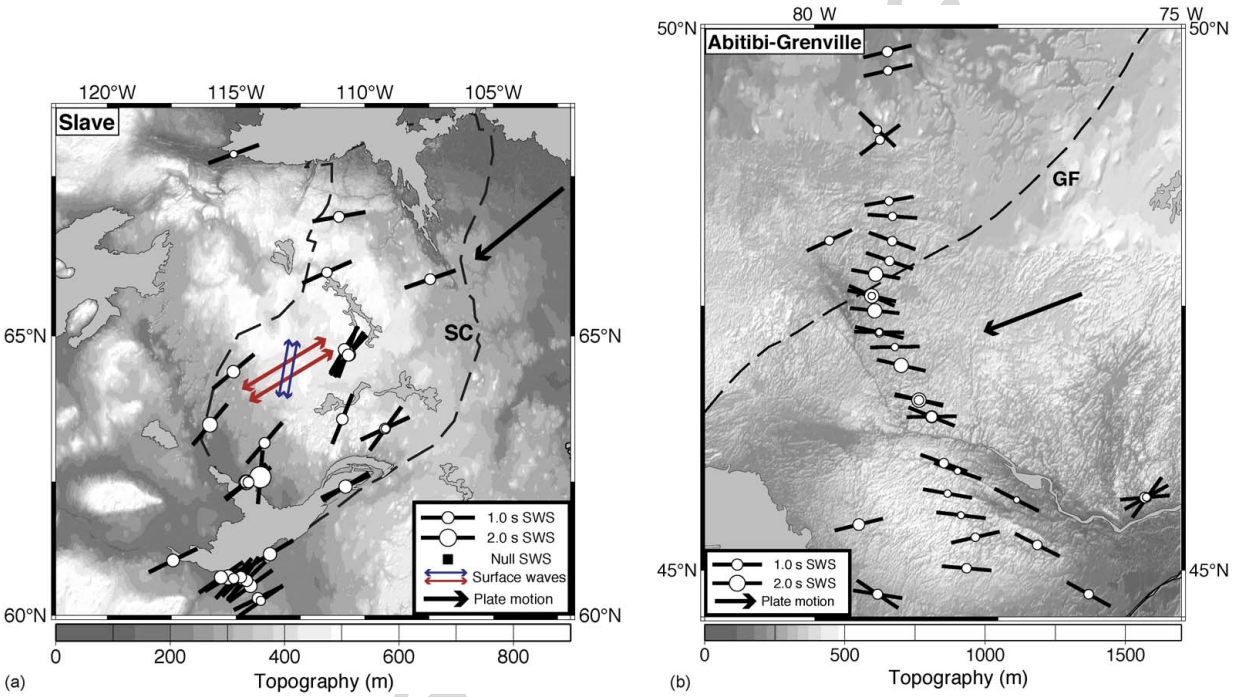

Fig. 4. Summary of published azimuthal anisotropy results for parts of the Canadian Shield. See text for list of individual studies represented in this figure. (a) Results for the Slave craton region. Dashed line denotes approximate outline boundary of Slave craton (SC). Shear wave splitting fast polarization directions are denoted by single black bars; open circles are scaled to splitting time values. Surface wave fast directions are shown by long double arrow (lithospheric mantle average) and short double arrow (crustal average). Large black arrow denotes absolute plate motion direction (Gripp and Gordon, 2002). In this region, seismic anisotropy appears to be primarily controlled by fabric oriented in the direction of plate motion in both the lithospheric keel and sublithospheric mantle as defined by the cratonic boundary. (b) Results for the Abitibi/Grenville region. Dashed line denotes approximate location of Grenville Front (GF). Shear wave splitting fast polarization directions are denoted by black bars; open circles are scaled to splitting time values. Large black arrow denotes absolute plate motion direction (Gripp and Gordon, 2002). In this region, seismic anisotropy appears to be controlled by a combination of lithospheric fabric and sublithospheric fabric generated by flow around and beneath the regional lithospheric keel as defined by regional surface wave images.

Author's copy

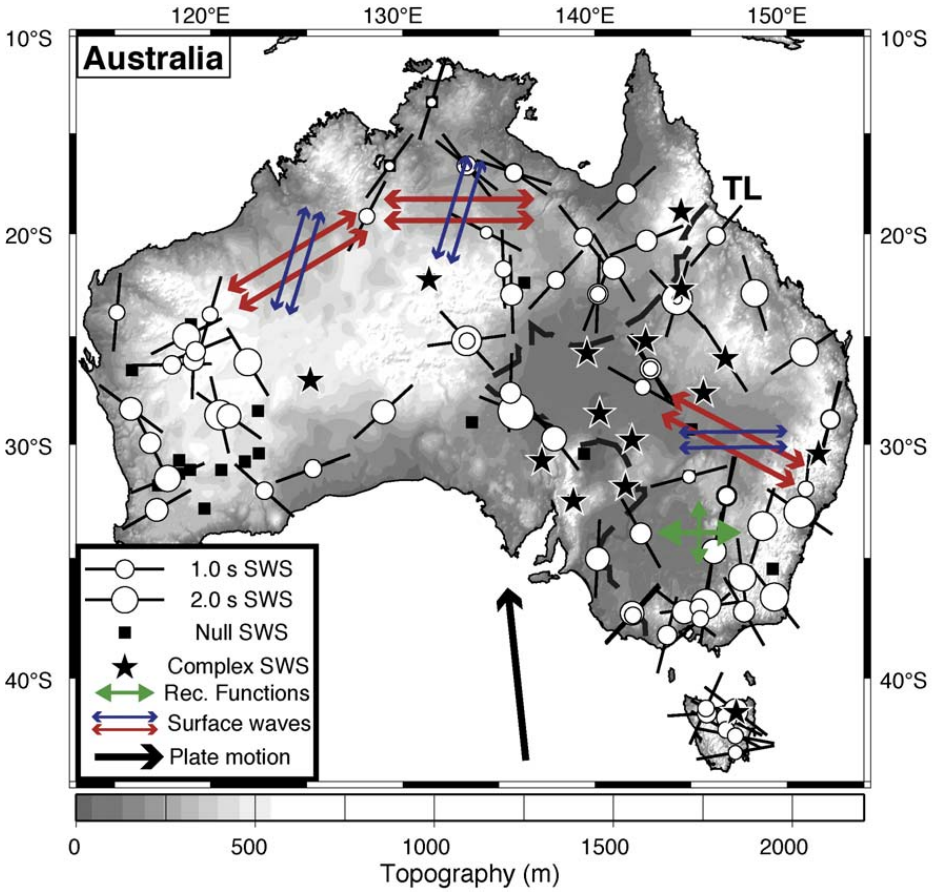

Fig. 5. Summary of published azimuthal anisotropy results for Australia. See text for list of individual studies represented in this figure. Dashed line denotes surface boundary of Tasman Line (TL) from Shaw et al. (1996). Shear wave splitting fast polarization directions are denoted by single black bars; open circles are scaled to splitting time values; null shear wave splitting measurements are shown by black boxes; complex shear wave splitting parameters are denoted by black stars. Receiver function fast polarization directions are denoted by thinner single arrow (crustal anisotropy) and thicker single arrow (lithospheric anisotropy). Surface wave fast directions are shown by thicker double arrow (average at 200 km depth) and thinner double arrow (average at 100 km depth). Large black arrow denotes absolute plate motion direction (Gripp and Gordon, 2002). In this region, seismic anisotropy appears to be controlled by a combination of lithospheric fabric and sublithospheric fabric generated by flow around and beneath the regional lithospheric keel as defined by the Tasman Line.

4.1. Eastern North America

We first turn to eastern North America, the subject of several seismic anisotropy studies over the past two decades. Summaries of findings presented here are plotted in Figs. 3 and 7. The oldest interior parts of the lithosphere in this region have remained stable for >2.5 Ga, while regions to the east are much younger in age (Grenville Province, 1.3–1.0 Ga; Appalachians, <1.0 Ga) (Hoffman, 1989). Rifting in the late Precambrian preceded compressional events in the late Paleozoic that formed the Appalachians (Kamo et al., 1995). More rifting events followed in the late Triassic and early Jurassic (Klitgord et al., 1988), producing the clear range of tectonic boundaries observed today. The absolute plate motion for this region averages S70W at a rate of ~3.1 cm/year (Gripp and Gordon, 2002).

A host of shear wave splitting results is available from several temporary seismic arrays deployed in this region, including APT89, ABBA, MOMA, POLARIS, and TWIST. These data are supplemented by those from permanent stations of the IRIS Global Seismic Network (GSN), the United States National Seismograph Network (USNSN), and GEOSCOPE stations. Shear wave splitting studies of the region are extensive (Ansel and Nataf, 1989; Vinnik et al., 1989, 1992; Silver and Chan, 1991; Silver and Kaneshima, 1993; Bostock and Cassidy, 1995; Levin et al., 1996, 1999; Silver, 1996; Barruol et al., 1997; Kay et al., 1999a,b; Fouch et al., 2000; Rondenay et al., 2000; Eaton et al., 2004a). Details of the patterns of these studies are discussed in Fouch et al. (2000); we therefore only summarize them here.

For stations located above the southern and central portions of the lithospheric keel as imaged by van der Lee

Author's personal

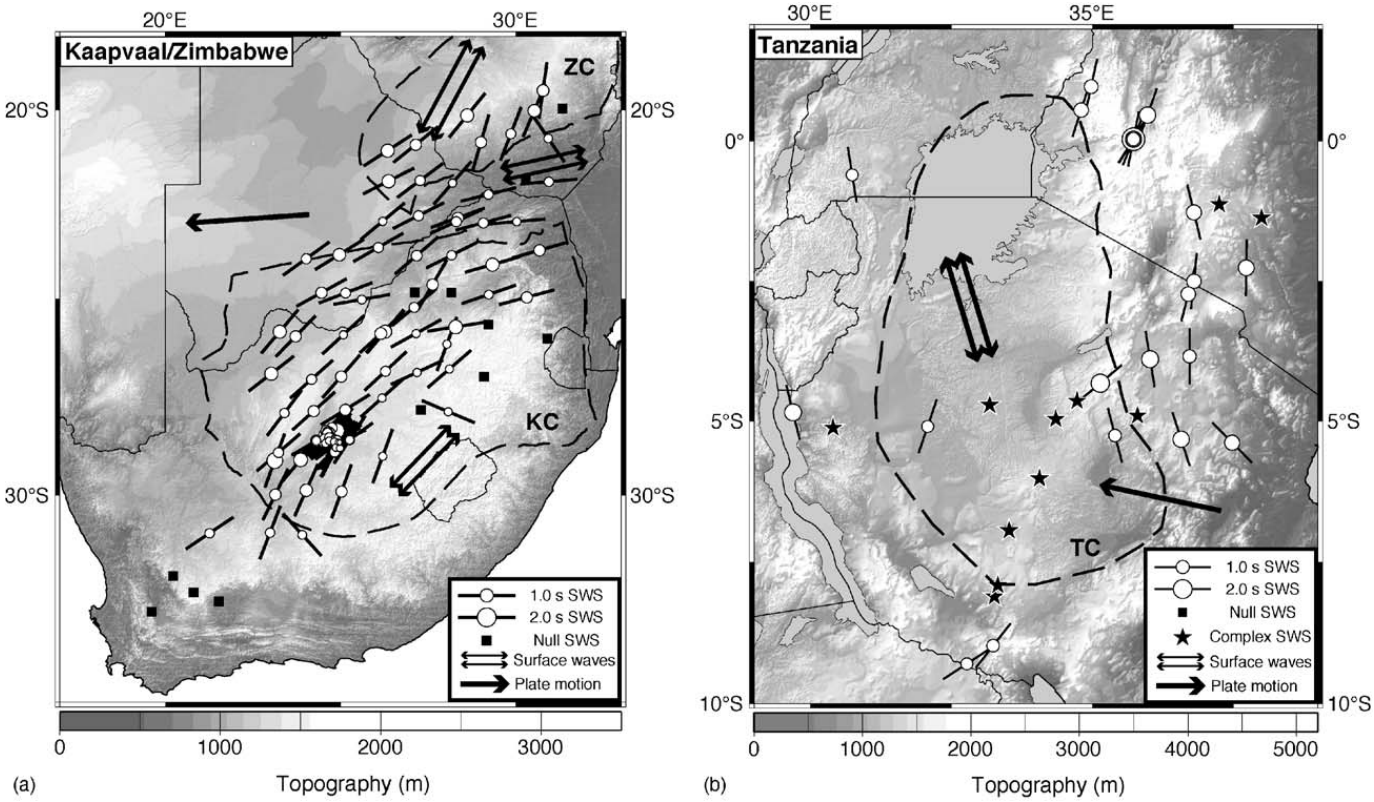

Fig. 6. Summary of published azimuthal anisotropy results for southern Africa. See text for list of individual studies represented in this figure. (a) Results for the Kaapvaal/Zimbabwe region. Dashed lines denote surface boundary of the Kaapvaal craton (KC) and Zimbabwe craton (ZC). Shear wave splitting fast polarization directions are denoted by single black bars; open circles are scaled to splitting time values; null shear wave splitting measurements are shown by black boxes. Surface wave fast directions shown by double black arrow. Large black arrow denotes absolute plate motion direction (Gripp and Gordon, 2002). In this region, seismic anisotropy appears to be controlled primarily by lithospheric fabric. (b) Results for the Tanzania region. Dashed line denotes surface boundary of the Tanzania craton (TC). Shear wave splitting fast polarization directions are denoted by single black bars; open circles are scaled to splitting time values; null shear wave splitting measurements are shown by black boxes; complex shear wave splitting parameters are denoted by black stars. Surface wave fast directions shown by double black arrow. Large black arrow denotes absolute plate motion direction (Gripp and Gordon, 2002). In this region, seismic anisotropy appears to be controlled by lithospheric fabric and sublithospheric fabric generated by impeded flow around the regional lithospheric keel as defined by the cratonic boundary.

and Nolet (1997), fast polarization directions are nearly parallel to the direction of APM, with some significant deviations for stations of the APT89 array (Silver and Kaneshima, 1993), where fast directions are not consistent over lateral scales of 70 km and less. We note, however, that shear wave splitting at most of the APT89 stations was determined using only one or two events, which may explain a portion of the variability. For stations S and SE of the lithospheric keel, fast directions are roughly tangent to the keel and appear to wrap around its lateral margins. Stations located within a divot in the keel appear to be oriented roughly E–W, with some lateral variations over short spatial scales. This region also exhibited more complexity in shear wave splitting as elucidated by Levin et al. (1999), who found that a two-layer model of anisotropy best fit the data for two permanent stations in the northeastern U.S.

Additional constraints on seismic anisotropy for this region are also available. Pn anisotropy measurements for this region are limited (e.g., Smith and Ekström, 1999), but where available, possess ~N–S fast directions for regions SE of the lithospheric keel, roughly opposite those fast directions from shear wave splitting. Conversely, Smith and Ekström determined ~E–W fast directions for eastern regions near the keel divot, parallel to shear wave splitting fast polarization directions. Vinnik et al. (2005) used receiver functions at the MOMA array to image a clear seismic boundary at 200 km depth, but determined that this discontinuity is not a first-order anisotropic boundary. Gaherty (2004) also used Love and Rayleigh phase delay differences across the MOMA array to obtain a model of radial anisotropy in the lithosphere combined with azimuthal anisotropy located in the sublithospheric mantle. Similarly, Li et al. (2003) used the two-plane wave analysis approach to sample a region of the northeastern U.S. and also found that significant azimuthal anisotropy must exist at depths greater than 200 km.

Author's personal

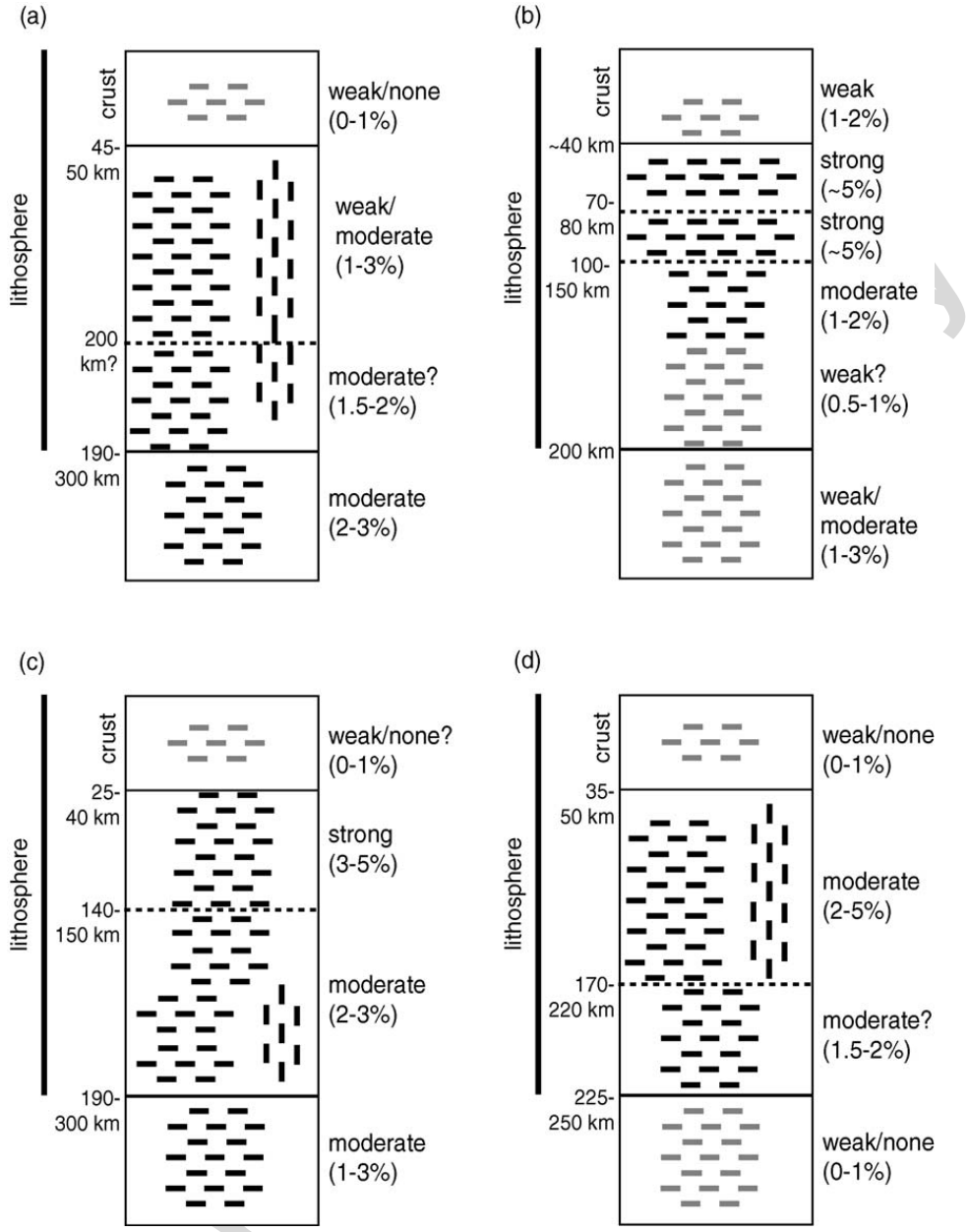

Fig. 7. Summary of seismic anisotropy in lithosphere/asthenosphere from each of the four case studies presented in this review. For each panel, left column values are depth to seismically-inferred boundary; right column is % anisotropy inferred from range of studies. Azimuthal anisotropy is denoted by horizontal bars; radial anisotropy is denoted by vertical bars. All regions show distinct evidence for lithospheric anisotropy and likely signs of crustal anisotropy. All regions except southern Africa show clear evidence for sublithospheric anisotropy. Radial anisotropy is prevalent in all regions except the Canadian Shield. For two subregions of the Canadian Shield, results are summarized for both. (a) Eastern North America; (b) Canadian Shield; (c) Australia; (d) Southern Africa.

These investigations point to a range of structures involving anisotropic layers in both the lithosphere and sublithospheric mantle across the region. We note that at present, however, very few constraints regarding crustal anisotropy exist for this region. The upper mantle component is in some cases dominated by lithospheric fabric (e.g., in the thickest parts of the keel), and in others by a combination of lithospheric and asthenospheric fabric (e.g., near the boundaries of the keel).

The investigations presented in this section point to a complex structure involving anisotropic layers in the lithospheric mantle and asthenosphere (sublithospheric mantle). The upper mantle component of anisotropy is in some case dominated by lithospheric fabric (e.g., in the SE and interior regions of the Shield), and in others by a combination of lithospheric and asthenospheric fabric (e.g., Slave and perhaps other regions at the periphery of the Shield).

4.2. Canadian Shield

We now turn our attention to the Canadian Shield, the object of numerous geophysical investigations via several major Earth science initiatives including Lithoprobe, POLARIS and IRIS-PASSCAL experiments. Summaries of findings presented here are plotted in Figs. 4 and 7. It is here that Silver and Chan (1988) presented SKS splitting results indicating the presence of seismic anisotropy in the continental lithosphere that were possibly of fossil origin. Anisotropy studies of the patchwork of Archean and Proterozoic terranes that make up the Canadian Shield have yielded results as varied as its building blocks; we therefore do not wish to provide an exhaustive review of this body of work here. Rather, we highlight case studies where integrated interpretations have helped to constrain the depth extent and underlying causes of anisotropy. Accordingly, we focus on two geographical areas: the Slave craton and the Abitibi-Grenville region.

4.2.1. Slave Province

The Slave Province is a small Archean craton located in the northwest corner of the Canadian Shield. It is flanked by two Proterozoic orogens, the Thelon orogen to the east and the Wopmay orogen to the west (Hoffman, 1989; Bowring and Grotzinger, 1992). Although small in areal extent, the Slave indisputably possesses cratonic roots (e.g., Hoffman, 1990) whose uncommon structure appears to reflect several stages of assembly and disruption at least in part associated with the docking of neighboring terranes. Several key investigations in the last decade have utilized receiver functions and shear wave splitting in SKS phases to yield new constraints on seismic anisotropy beneath the region (Fig. 4a). In a landmark receiver function survey, Bostock (1997, 1998) used 10 years of data from the permanent Yellowknife seismic array to conduct an azimuthal analysis of Ps waves converted at mantle discontinuities beneath the southern Slave. This analysis revealed a well-developed mantle stratigraphy extending from the Moho down to the mantle transition zone. Two main anisotropic horizons were imaged at 70–80 km and 120–150 km depth. Modeling results show that the layers are strongly anisotropic (±5%) and are separated from upper/lower isotropic media by sharp boundaries that are 700 m or less thick. Bostock (1998) extrapolated these structures westward to connect them seismic reflection images of suture zones and associated east-dipping mantle reflectors underlying the Proterozoic Wopmay orogen (Cook et al., 1999). He interpreted the layers as evidence for lithospheric assembly by shallow subduction and underplating, where the anisotropic layers represent eclogitized oceanic crust. This structural model is supported by recent receiver function observations by Snyder et al. (2004), which indicate that complex lithospheric layering appears to extend laterally throughout the entire Slave craton. At shallower depths, Bank and Bostock (2003) found evidence for lower crustal anisotropy beneath the SW Slave craton by applying 1-D Born scattering inversion to Moho conversions. This signal may be attributed to large-scale regional N–S trending crustal folds mapped by Bleeker et al. (1999).

The first regional shear wave splitting study of the Slave craton was undertaken by Bank et al. (2000), who analyzed data from a 2-year reconnaissance deployment of 13 broadband stations. Average SKS splitting measurements from these stations were fairly uniform throughout the Slave, with fast polarization directions oriented $\sim$N60E $\pm$ 15° and average delay times of $\sim$1.0 s, indicative of a mantle fabric primarily influenced by North American present-day plate motion. More recently, Snyder et al. (2003) reevaluated data from these stations using an additional 3 years of waveform data and found similar results. Of more importance, however, Snyder et al. (2003) also analyzed SKS splitting from a semi-permanent seismic station located in the central Slave craton to further characterize seismic anisotropy beneath the region. Comprehensive SKS azimuthal coverage yielded evidence for two-layer azimuthal anisotropy, one representing plate motion (N50E, similar to that observed by Bank et al., 2000) and another thinner layer, possibly aligned with the regional crustal folding discussed above. Eaton et al. (2004b) reported similar SKS splitting results for stations in the SE Slave. However, coincident MT measurements suggest that the lower anisotropic layer may be confined to the lithospheric mantle in that region, though we note that the relationship between MT and seismic measurements of anisotropy are still not well known (e.g., Simpson, 2002). Preliminary results from surface wave analyses in the Slave craton (e.g., Chen et al., 2005) support both models, requiring seismic anisotropy to be partitioned between the lithosphere and asthenosphere.

4.2.2. Abitibi-Grenville region

The second region of interest is situated in the SE Canadian Shield and encompasses a variety of late-Archean to Paleozoic geological terranes (Fig. 4b). The northern region comprises the Archean Superior Province of the Canadian Shield, while the southern portion of the study area is within the Grenville Province, which is composed of Proterozoic and reworked Archean

Author's personal copy

rocks. The Superior and Grenville Provinces are separated by the continuous SW–NE trending Grenville Front, a major crustal discontinuity that is the locus of important uplift, change in metamorphic grade, faulting and mylonitization (Rivers et al., 1989; Rivers, 1997).

The SE Canadian Shield has been carefully investigated thanks in large part to the Lithoprobe Abitibi-Grenville transect running through the region (Clowes, 1997). An interesting note is that this region was the first where coincident seismic, magnetotelluric and xenolith analyses were employed simultaneously to characterize mantle anisotropy. Magnetotelluric surveys first revealed the presence of upper mantle electrical anisotropy (Kellett et al., 1994; Mareschal et al., 1995), which was attributed to interconnected grain boundary graphite precipitated from hydrothermal activity during Archean tectonic events. MT phase analyses yielded a maximum conductivity azimuth of N80°E, and showed that the anisotropic region was confined to depths of ~50–150 km. Shear wave splitting analysis later uncovered the existence of similar seismic anisotropy, with regionally averaged splitting parameters of $\phi = 101 \pm 10^\circ$ and $\delta t = 1.46 \pm 0.21$ s (Sénéchal et al., 1996; see also Rondenay et al., 2000a,b). The similarity in principal directions between electrical and seismic anisotropies (within a systematic ~20° obliquity) led Sénéchal et al. (1996) to suggest a common genetic link. Moreover, considering the depth constraint provided by MT results and that the principal directions are aligned with the orientation of major deformation zones in the area, splitting results were attributed to "frozen-in" lithospheric fabric. Ji et al. (1996) further interpreted the systematic ~20° obliquity between the two anisotropies as a kinematic indicator manifesting dominantly east–west dextral shearing during the last episode of deformation. Using SKS delay times from Sénéchal et al. (1996) and an S-velocity anisotropy of 3.2% inferred from local xenoliths samples, Ji et al. (1996) estimated the thickness of the anisotropic layer to be ~200 km. Contrasting layer thicknesses for electrical (100 km) and seismic (200 km) anisotropy can be reconciled if the stability field of the conductive phase (i.e., graphite) extends to a maximum depth of approximately 150 km (Ji et al., 1996; and references therein). Seismic anisotropy could then extend to greater depths within the thick cratonic lithosphere.

The investigations presented in this section, as well as other studies conducted elsewhere in the Canadian Shield (e.g., Kay et al., 1999a,b; Bökelmann, 2002; Bank and Bostock, 2003; Musacchio et al., 2004), all point to a complex structure involving anisotropic layers at all levels of the crust, lithospheric mantle and asthenosphere (sublithospheric mantle). The crustal component is almost ubiquitous, but contributes the smallest amount of anisotropic signal due to the limited depth extent over which coherent fabric is present. The upper mantle component is in some case dominated by lithospheric fabric (e.g., in the SE and interior regions of the Shield), and in others by a combination of lithospheric and asthenospheric fabric (e.g., Slave and perhaps other regions at the periphery of the Shield).

4.3. Australia

The Australian continent is another excellent natural laboratory to test hypotheses for the origin and significance of anisotropy. Summaries of findings presented here are plotted in Figs. 5 and 7. Australia is a collage of well-defined terranes whose ages grow older from east to west, from Phanerozoic to Proterozoic to Archean. Moreover, it is the fastest moving continental mass with an average speed of ~8 cm/year approximately to the N (Gripp and Gordon, 2002). In the past ~10–15 years, Australia has been the object of important seismological scrutiny thanks to a mounting coverage of permanent stations of the GSN and GEOSCOPE networks and the extensive regional coverage afforded by the SKIPPY project (van der Hilst et al., 1994). Seismic anisotropy beneath the region was investigated using shear wave splitting (Vinnik et al., 1992; Clitheroe and van der Hilst, 1998; Özalaybey and Chen, 1999; Heintz and Kennett, 2005), combined body/surface waves analyses (Gaherty and Jordan, 1995; Gaherty et al., 1999), RF analyses (Girardin and Farra, 1998), and surface wave tomography (Debayle, 1999; Debayle and Kennett, 2000a,b; Simons et al., 2002, 2003).

Shear wave splitting analyses conducted on Australian data have produced rather enigmatic observations, with many stations returning consistently null results (Vinnik et al., 1992; Özalaybey and Chen, 1999) and others showing signs of weak, frequency-dependent anisotropy (Clitheroe and van der Hilst, 1998). Clitheroe and van der Hilst (1998) determined split times of 0.3–0.6 s for stations in the Precambrian terranes of central Australia that are only observable at high frequencies. Fast polarization directions are generally correlated with, and therefore attributed to, the trend of large-scale crustal structures rather than APM. However, based on SKS/SKKS observations from permanent stations and Fresnel zone arguments, Özalaybey and Chen (1999) argue that the transverse signal observed only occasionally at high-frequency is due to local scattering originating in the lower mantle rather than upper mantle anisotropy. Heintz and Kennett (2005) performed a

Author's personal copy

continental-scale survey of shear wave splitting and also found fast polarization directions that correlated to first order with primary crustal structures and variations in splitting parameters over lengths scales of <50 km, suggesting that the bulk of the anisotropy resides in the lithosphere. They do not rule out the possibility that sublithospheric structure contributes to the splitting signal.

Based on RF analyses from a permanent station in SE Australia, Girardin and Farra (1998) suggested an alternative explanation for the null and/or weak splitting results. They found evidence for two-layer anisotropy and showed that the birefringence effects from the two layers may effectively cancel each other when sampled by SKS phases evaluated for shear wave splitting. Moreover, they found that the upper layer (40–140 km depth) has a fast axis oriented E–W that is attributed to fossil lithospheric fabric acquired during a Paleozoic extensional event, whereas the lower layer (140–190 km depth) has a fast axis oriented approximately N–S and is representative of present-day plate motion.

Surface wave analyses conducted in the Australian continent corroborate the findings of Girardin and Farra (1998) and extend them to the entire continental mass (e.g., Debayle and Kennett, 2000a,b; Simons et al., 2002). They find laterally variable anisotropic parameters in the upper lithosphere (0–150 km depth), with a correlation between regional lithospheric structures and anisotropic trends. At greater depth, anisotropy is detected down to ~250 km but its behavior is more uniform across the continent, with fast axes generally oriented in the N–S direction and representative of present-day plate motion of the Australian continent. These results are further constrained by measurements of mechanical anisotropy obtained by Simons et al. (2003), who demonstrate a correlation between isostatic anisotropy and fast polarization directions in the upper ~150 km of the lithosphere. The interpretation of this correlation is that ancient strain weakens the lithosphere while developing LPO.

To summarize, the Australian continent is similar to the Canadian Shield in that they both appear to be anisotropic at all levels, from the lower crust to the base of the lithosphere, and perhaps in the asthenosphere. This appears to hold true despite the anomalous shear wave splitting results observed in Australia, which are probably due to the competing effects of the various anisotropic layers.

4.4. Southern Africa

Like the Canadian Shield, southern Africa provides an exceptional opportunity to examine continental seismic anisotropy in a region that has been well sampled seismically and also contains numerous samples of mantle rocks. Summaries of findings presented here are plotted in Figs. 6 and 7. This case study focuses on the Kaapvaal/Zimbabwe and Tanzanian cratons, two regions that have benefited from extensive seismic sampling. Seismic data from global GSN and Geoscope stations have been utilized in tandem with recent temporary broadband seismic arrays deployed in the region, including the Southern Africa Seismic Experiment (Carlson et al., 1996) and the Tanzania Broadband Seismic Experiment (Nyblade et al., 1996).

The Archean Kaapvaal and Zimbabwe cratons form the nucleus of southern Africa (Fig. 6a). The Kaapvaal craton is comprised of a mosaic of distinct geologic terranes covering more than 10^6 km^2, with the oldest units generally in the eastern part of the craton and the youngest in the western part (de Wit et al., 1992). These terranes of disparate geologic histories were assembled over a 1 Ga period from early late Archean (~3.6–2.6 Ga) (de Wit et al., 1992; de Wit and Hart, 1993; Carlson et al., 2000). The plate motion direction for the African plate is not well constrained, in part since plate speeds are nearly the slowest in the world (no more than 1 cm/year in the vicinity of southern Africa) (Gripp and Gordon, 1990, 2002). The Tanzanian craton, while less extensively studied, is also Archean in age and is surrounded by several shear belts marking strike-slip and convergent deformation during cratonic amalgamation (e.g., Cahen et al., 1984).

Petrofabric analyses of mantle xenoliths from the Kaapvaal craton at the Bultfontein kimberlite near Kimberley provide direct evidence of a source for seismic anisotropy. These samples exhibit distinct lattice-preferred orientations with an average intrinsic shear wave anisotropy value of ~1.7% (assuming a vertical foliation plane) (Ben-Ismaïl et al., 2001). Samples from several nearby regions (Ben-Ismaïl et al., 2001) confirm that mantle anisotropy exists down to at least ~145 km and likely deeper. Similarly, Vauchez et al. (2005) used samples from Labait volcano within the Tanzania craton to determine a range of shear wave polarization anisotropies between 2.8% and 8.3% and a general increase in anisotropy with depth to at least 140 km. These constraints are critical in the evaluation of the strength and depth extent of seismic anisotropy in these cratonic regions.

4.4.1. Kaapvaal/Zimbabwe cratons

The ongoing debate regarding the origin of continental seismic anisotropy was in many ways instigated by shear wave splitting analyses from southern Africa. Early

Author's personal copy

shear wave splitting results from Vinnik et al. (1995, 1996) suggested that seismic anisotropy beneath southern Africa is primarily related to shear in the mantle induced by plate motion direction. As noted above, however, APM is not well constrained in this region. Silver et al. (2001) observed mantle anisotropy throughout the Western Kaapvaal, Zimbabwe Craton, and Limpopo belt but found it to be only weakly present in the eastern Kaapvaal Shield and off-craton to the south and west. The values of ϕ exhibit systematic spatial variations. In the southwestern Kaapvaal they are roughly NNE–SSW, rotate to NE–SW further north, and to nearly EW in the northeastern part of the craton, including the Limpopo belt. Just north of the Limpopo, there are several stations in the vicinity of the Great Dyke with ϕ values oriented NNE–SSW. Values of ϕ range from about 0° to 80° (clockwise from north), and δt values for the entire region are small. Where detected, δt is roughly half of the global average of 1.0 s, and splitting was not detected at ~25% of the stations.

A study by Fouch et al. (2004b) used the densely-spaced Kimberley Telemetered Array (~5 km station spacing) located in the heart of the Kaapvaal craton to discover fast polarization directions oriented $46 \pm 3°$ and nearly identical across the 40 km × 60 km array. More importantly, significant splitting time variations exist over spatial scales of <50 km, which also suggests a lithospheric source based on Fresnel zones for these SKS phases. Assuming that anisotropy is uniformly distributed over a 115 km thick mantle layer (i.e., 150 km maximum depth of anisotropy with a 35 km thick isotropic crust), shear wave splitting results suggest a maximum strength of ~2.8% anisotropy in the mantle, and an average strength of ~1.8% in this region. These results were corroborated by analyses of relative delay times for SKS and PKP phases, which detect a rapid change in anisotropy over <50 km.

Average crustal anisotropy values from stacked Moho Ps phase conversions suggest that the crustal component of anisotropy generates a shear wave splitting time of no more than 0.2 s at KTA stations (Gao, personal communication, 2002). The very small splitting time values derived from this analysis prevented a determination of well-constrained fast directions. This result suggests that the contribution to δt is primarily from the mantle, as the crustal component is estimated to be no more than 20% of the total SKS splitting time (Silver et al., 2001).

The inference that seismic anisotropy exists primarily in the lithosphere beneath southern Africa is corroborated regionally by surface wave studies of radial and azimuthal anisotropy (e.g., Freybourger et al., 2001; Saltzer, 2002). First, the magnitudes of anisotropy inferred from the surface and body wave datasets are compatible (e.g., Freybourger et al., 2001; Saltzer, 2002), though the anisotropy found from surface wave studies is radial in nature. Integrating the predicted shear wave splitting delay time using the surface wave model yields an estimate of 0.6 s, nearly identical to the average splitting delay time (Silver et al., 2004), but no detectable azimuthal anisotropy when averaged over the entire dataset. The average depth extent of the anisotropy inferred from these surface wave analyses indicates that it is primarily of mantle origin and is located to depths no greater than 220 km, well within the lithospheric keel as imaged by both body wave tomography (James et al., 2001; Fouch et al., 2004a) and surface waves (Qiu et al., 1996; Ritsema and van Heijst, 2000; Freybourger et al., 2001; Saltzer, 2002). The location of anisotropic boundaries within the lithospheric mantle is also corroborated by a detailed analysis of receiver functions derived by the Kimberley Telemetered Array (Rondenay and Fouch, in preparation).

4.4.2. Tanzania

Fewer studies have been performed for the Tanzanian craton, most significantly due to a smaller volume of data for the region particularly relative to the Kaapvaal/Zimbabwe region (Fig. 6b). An early study of permanent broadband stations NE of the craton found fast polarization directions oriented approximately N20°W and splitting times near 1.0 s (Barruol and Ben-Ismaïl, 2001). Walker et al. (2004) used data from a temporary broadband seismic experiment to find clear evidence of shear wave splitting in the vicinity of the Tanzanian craton that suggests structural complexity (i.e., multiple layers of anisotropy) in the region. Around the edges of the craton, they found fast polarization directions that mimic the shape of the craton and lithospheric keel boundaries as imaged by Nyblade et al. (2000), and splitting times that ranged from 0 s to ~2.0 s. Stations within the keel tended to exhibit more complexity in splitting behavior. Their results clearly indicate the presence of lithospheric anisotropy, but the complexity in some regions suggests a component of sublithospheric anisotropy possibly generated from lithospheric plate motion. Weeraratne et al. (2003) used surface waves to infer shear wave fast polarization directions that average NNW/SSE, projected splitting times of ~0.4 s, and therefore relatively weak azimuthal seismic anisotropy. We note that this study may underestimate the regional strength of anisotropy due to averaging of cratonic regions next to active rifting areas.

To summarize, crustal anisotropy beneath southern Africa appears to be weak at best, while overall litho-

Author's personal copy

spheric anisotropy is also weak relative to the global average (e.g., Silver, 1996). Sublithospheric anisotropy does not appear to exist beneath the Kaapvaal/Zimbabwe region, but may exist around the Tanzania craton. We note that the Tanzanian region is significantly more complicated tectonically than the Kaapvaal because it is juxtaposed to the active East African continental rift margin and may be actively experiencing mantle deformation due to a plume beneath the craton (e.g., Walker et al., 2004).

4.5. Summary and implications

With the exception of the Kaapvaal/Zimbabwe region of southern Africa, all regions discussed here show clear evidence for a combination of both lithospheric and sublithospheric seismic anisotropy (Fig. 7). Given the possible causes of anisotropy, this result should not be surprising, as one would expect fabric to develop preferentially at all levels within and near the base of rigid continental masses.

A fabric that generates seismic anisotropy likely reflects the complex tectonic evolution of continental lithosphere. Regional correlations between seismic anisotropy and surface geologic features have been examined in detail (e.g., Silver, 1996 and references therein). The reader is referred to this body of work for a more complete treatment of this issue. Azimuthal anisotropy correlated with plate motion is also a logical consequence of plate tectonics. Debayle et al. (2005) noted that APM direction and azimuthal anisotropy derived from a global surface wave inversion correlate nearly everywhere beneath Australia, but only locally beneath North America and the Canadian Shield, and not at all beneath southern Africa. They suggest that the difference between Australia other regions is due to the high speed of the Indo-Australian plate, which induces an exceptionally coherent fabric at the base of the lithosphere. The corollary to this hypothesis is that low speed plates such as the African plate would induce very little fabric in the sublithospheric mantle, consistent with most seismic anisotropy observations for the region. While the study by Debayle et al. (2005) does not address the complexity of continental keel morphology in changing mantle flow patterns (e.g., Fouch et al., 2000), the global correlation between plate velocity and seismic anisotropy remains important. An additional constraint consistent across most regions is the observation of radial anisotropy via surface wave analyses. Radial anisotropy does not strongly affect shear wave splitting results, potentially causing an underestimate of the total anisotropy in a region. We also note that other continental regions, such as parts of Europe (e.g., Bormann et al., 1996) and South America (e.g., James and Assumpçao, 1996), also appear to require a combination of anisotropic zones in the lithosphere and sublithosphere. A combination of fabric in both components of the plate tectonic system therefore seems to be not the exception, but rather the rule for most stable continental interiors.

A single interpretation of these collective findings is still under debate. For instance, the range of the depth distribution of seismic anisotropy for many continental regions is consistent with a model in which lithospheric mantle is strongly coupled to the lithosphere, but that sublithospheric shearing rates are slow due to high viscosities in this depth region. Alternatively, a more likely scenario is that lithospheric plates are only partially coupled to the mantle beneath them. In this model, variable degrees of coherent sublithospheric anisotropy could be explained primarily by high or low degrees of shearing due to present-day plate velocity variations.

To further examine these competing models, it is clear that data that provide significantly improved constraints on the lateral and the depth distribution of anisotropy are required to determine clearly the relative strengths of anisotropy in lithosphere and sublithospheric mantle. In particular, seismic anisotropy imaging efforts from future seismic experiments should sample regions for extended periods of time to improve resolution of 3-D variations in seismic anisotropy. These improved limits would also comprise an important range of boundary conditions in numerical models of plate interactions that tend to explore only end-member cases of coupling between plates and the mantle underlying them.

5. Future directions

A common limitation to most techniques reviewed in Section 3 is that the problem being solved is underdetermined (or more accurately, mixed-determined). This problem results in important tradeoffs between solutions for various anisotropic parameters. Consequently, it appears that most individual techniques described above have been pushed to their limits, with few exceptions. In some regions, increased data coverage might reduce uncertainties to some degree, but some anisotropic parameters will remain unconstrained even if data coverage was truly exhaustive. For example, shear wave splitting in SKS phases is inherently poorer at constraining the depth extent of anisotropic structure than surface wave analyses. Crustal anisotropy likely plays an important role in most observations of anisotropy, particularly in body wave, but is also not well characterized in most

Author's personal copy

regions (e.g., Savage, 1999). Similarly, source–receiver geometries and the necessity to analyze seismic phases from a limited range source distances (e.g., Wysession, 1996; Chevrot, 2000) mandates that seismic anisotropy simply cannot be well imaged beneath some continents (and generally, some regions of Earth) with existing techniques.

In this context, the key to further advancement in constraining seismic anisotropy must lie in the development of new, innovative methods in tandem with the integration of existing analysis techniques and datasets. Below, we present a roadmap of potential innovation and implementation of several approaches that show promise in achieving this goal. We emphasize that the following discussion does not include an exhaustive list of possible methodologies, but rather presents our current view of how to improve imaging of continental seismic anisotropy.

5.1. Emerging methods

Several recently developed techniques show promise to join the well-established methods described in Section 3 as standard analysis methods. We briefly discuss three of these incipient methodologies.

5.1.1. P polarizations

Measurements of P polarizations (Ppol) are still in early stages of development for mantle anisotropy studies (e.g., Schulte-Pelkum et al., 2001), though this technique has been used in crustal studies of seismic anisotropy since the mid-1990s (e.g., Bökelmann, 1995). In this particle motion analysis method, polarizations of teleseismic P-waves are measured and examined for deviations from vertical–radial plane (sagittal) polarization. Following inversion for regional correlations in polarization anomalies, maps are produced of P-wave fast polarization directions and anisotropic magnitudes. The primary advantage of Ppol analysis is that it provides unique constraints on seismic anisotropy relative to the other body wave techniques described above, yet eliminates some of the small-scale variations that may plague other studies. A primary disadvantage of this approach is that the cause of the anomalous polarizations could be due to isotropic structure such as scatterers. In addition, Ppol has limited resolution to lateral and depth variations of anisotropic parameters on the order of 1 wavelength, or ~250 km. We note, however, that this methodology is currently being utilized in regional analyses for mantle structure and should prove to be an important regional constraint as it is further improved (Becker et al., 2006a,b).

5.1.2. Removal of free-surface and lowermost mantle effects

A significant issue with some methods used in seismic anisotropy imaging is the contamination of shear waves by crustal and free-surface interactions (e.g., multiples or scattering), particularly for seismic waves whose incidence angle is greater than ~35° (e.g., Keith and Crampin, 1977). This constraint is problematic in that it limits well-populated ranges of backazimuthal and incidence angles for many regions of the world. Additionally, this effect has led to spurious observations of shear wave splitting for regional S observations (e.g., Wookey et al., 2002) that were contaminated by shear-coupled P phases (e.g., Wookey and Kendall, 2004). Similarly, several studies in the literature have made use of shear phases that either significantly sampled D″ or diffracted along the core–mantle boundary (e.g., Levin et al., 1999) to infer upper mantle anisotropy. Given that the lowermost mantle is seismically anisotropic, phases sampling this region are also potentially contaminated by non-receiver side anisotropic structure. Efforts to provide tools that reduce these effects are underway (e.g., Wookey and Kendall, 2004), but continued work in this arena has the potential to significantly increase the volume of waveforms available for seismic anisotropy analysis.

5.1.3. Combined normal modes/surface waves/body waves

Although normal modes have been used independently to investigate inner core seismic anisotropy (e.g., Tromp, 1993; Beghein and Trampert, 2003; Ishii and Dziewonski, 2003), they are now becoming a tool for upper mantle studies when combined with constraints from body waves (e.g., Montagner and Kennett, 1996) or surface waves (e.g., Oda, 2005). These hybrid approaches yield anisotropic velocity models that are more robust than those obtained with traditional body or surface wave data alone, but require continued improvement to enable their use with the full range of datasets currently available such as those recorded by portable broadband arrays.

5.2. Future directions in seismic anisotropy imaging

Here we present some ideas of future avenues for improving the characterization of seismic anisotropy. The proposed methodologies are particularly tuned for the imaging of continental regions and assume that new, higher-resolution datasets will be available in the coming years. For instance, standard 1–2 year deployments of stations from the IRIS/PASSCAL and similar pools will continue to supply much of the necessary new data.

Author's personal copy

Similar experiments with short-term deployments, such as the combined transportable and flexible components of EarthScope's USArray (http://earthscope.org), will provide another unique data source. The POLARIS initiative (http://www.polarisnet.ca) is a proven case study in this regard, and has already developed the data infrastructure for new technique development. One of the most important needs, however, is for extended periods of data collection; portable long-term arrays such as NARS (http://www.geo.uu.nl/Research/Seismology/nars) are an excellent model to follow in this regard. We also note that the continued development of broadband seismic equipment that is cost-effective and simple to use presents an important opportunity to improve our ability to image seismic anisotropy on a range of scales.

We outline the new potential approaches organized under the following categories:

5.2.1. Array-based methods

While methods such as slant-stacking, beam forming, scattered wavefield imaging, and other array-based methods have been utilized in the past several years to image isotropic structure (e.g., Bostock et al., 2001; Rondenay et al., 2001; Rost and Thomas, 2002), few have exploited the benefits provided by array data to investigate seismic anisotropy. Current array methods that do consider anisotropy generally consider only anisotropic boundaries. These methods therefore typically cannot constrain the thickness or strength of anisotropic layers without modeling efforts to complement the observations (e.g., Bostock, 1998; Frederiksen et al., 2003). Given the improved geometry and density of current and future broadband arrays, we suggest that methods such as shear wave splitting will benefit from further development of array analysis-style stacking approaches to tease out otherwise weak or complex splitting signals (e.g., Gledhill and Gubbins, 1996). Additionally, relative shear wave splitting based on either a master station or multi-channel cross-correlation approach will likely become possible, and could provide better estimates of both lateral variations and the depth extent of anisotropy.

5.2.2. Combined methods

Integrated analyses of related seismic anisotropy datasets continue to be developed. While popular combinations include the integration of body and surface wave datasets (e.g., Montagner et al., 2000; Gung et al., 2003; Forsyth and Li, 2005), future inversions could include additional constraints from P polarizations, Pn anisotropy, and receiver function splitting. In a related vein, Gee and Jordan (1992) pioneered an approach that compares observed and synthetic seismograms of long-period S waves, S reverberations (SS, SSS, etc.), and Rayleigh/Love surface waves to measure generalized data functions representing velocity and anisotropic characteristics in the lithosphere. A range of later studies (e.g., Gaherty and Jordan, 1995; Katzman et al., 1998; Kato and Jordan, 1999; Gaherty, 2001) have demonstrated the utility of this technique. Future analyses using this approach could be extended to include other phases such as P and SKS since they are sensitive to different anisotropic regions. A somewhat similar approach could incorporate a modified form of the partitioned waveform inversion technique (Nolet, 1990) that would incorporate suites of radially and/or azimuthally anisotropic models. We note that the addition of every complementary dataset is obviously not feasible at once; rather, new datasets could be added to an inversion, and tradeoffs could be evaluated as these data are incorporated in the analysis.

5.2.3. Forward modeling methods

Methods that utilize forward modeling approaches as predictive tools to compare observations with data will continue to improve resolution of seismic anisotropy. For instance, one approach could be to assume a model's strength and geometry of anisotropy based on results from shear wave splitting analyses, and use this model to predict the response of other datasets based on back-azimuth and incidence angle. Simple tools such as an analytic traveltime equation technique (e.g., Frederiksen and Bostock, 2000) or a propagator matrix-type technique used in conjunction with raytracing (e.g., Fischer et al., 2000; Fouch et al., 2000; Hall et al., 2000) could be used. More complex predictive waveform modeling approaches that incorporate the effects of seismic wavefront sensitivity kernels (e.g., Fischer et al., 2005) should also be considered. Following predictions for a given dataset, families of viable anisotropic models could then be identified and refined in an iterative process (e.g., Sambridge, 1999a,b).

5.3. Multidisciplinary studies of continental anisotropy

As highlighted throughout this review, the interpretation of anisotropy as imaged from seismic data is a complex problem. We require a better understanding not only of the physical properties (i.e., mineral alignment or other fabric) directly responsible for seismic anisotropy, but also an improved knowledge of the deformational processes that generate this fabric. Here, we highlight the need for new constraints from mineral physics, petrology, and geodynamic modeling as examples of areas ripe

Author's personal copy

for breakthrough studies that will significantly aid in the interpretation of seismic anisotropy.

5.3.1. Mineral physics

As the primary constituent of the upper mantle, olivine has received the most attention for understanding LPO development, both from field samples (e.g., Kern, 1993; Ji et al., 1994; Kern et al., 1996; Long and Christensen, 2000; Soedjatmiko and Christensen, 2000; Ben-Ismaïl et al., 2001; Mehl et al., 2003; Tommasi et al., 2004b) and laboratory experiments (e.g., Karato, 1987; Zhang and Karato, 1995; Zhang et al., 2000). Pioneering studies on the effects of mantle hydration primarily examine the role of water in LPO of olivine (Jung and Karato, 2001), and will likely continue to be a major research thrust in the community. Similarly, the effects of partial melt on seismic anisotropy have recently begun to be characterized (e.g., Zimmerman et al., 1999; Holtzman et al., 2003). Given that other abundant mantle minerals such as clinopyroxene are inherently anisotropic and likely play a key role in fabric development (Ben-Ismaïl et al., 2001), a more complete understanding of LPO/SPO development and their implications for seismic anisotropy is required. A key contribution of mineral physics will therefore be the continuing development of methods by which more realistic mantle aggregates can be evaluated for seismic anisotropy constraints.

5.3.2. Numerical modeling of deformation and dynamics

Geodynamic models of mantle flow are key components in the interpretation of continental anisotropy. While flow models with realistic continental keels have been developed to investigate somewhat more complex flow patterns (e.g., Fouch et al., 2000), these families of models typically utilize simple mantle rheologies and rarely examine the relationship between lithospheric and sublithospheric coupling with respect to seismic anisotropy. We submit that 3-D models with appropriate lithospheric geometries and more realistic rheologies (e.g., temperature-dependent viscosity, partially hydrated mantle components) will enable the examination of flow systems that more accurately represent continental dynamics and can be more self-consistent with seismological models (e.g., Becker et al., 2006a,b).

5.3.3. Integration of related datasets

A more robust characterization of anisotropic parameters can be achieved not only through the integration of complementary seismic datasets (see Section 5.2), but also through the integration of seismic and other related geophysical data. For example, recent work has shown that measurements of electrical anisotropy from MT data can be used to constrain the depth extent of seismic anisotropy layers and to help interpret the source of this anisotropy (Ji et al., 1996; Eaton et al., 2004b; see also Section 4.2). Another noteworthy example involves the use of mechanical anisotropy measurements from gravity and topography data to determine the fraction of seismic anisotropy that can be attributed solely to lithospheric deformation (Simons et al., 2003; Simons and van der Hilst, 2003; Audet and Mareschal, 2004; see also Section 4.1). Although fully compatible parameterizations of seismic and other geophysical models may not be possible at this time, it has become clear that links do exist and should be exploited to constrain the interpretation of anisotropy beyond the limits imposed by seismology alone.

5.4. The need for a centralized seismic anisotropy repository

Finally, we address the importance of a centralized warehousing of data and results related to seismic anisotropy. While we currently maintain a simple database of published shear wave splitting parameters for core phases (http://geophysics.asu.edu/anisotropy/upper), we submit that establishing a modern, interactive seismic anisotropy data system for the Earth sciences community would further facilitate the marriage of data and models, and provide the necessary platform to facilitate homogenous datasets of seismic anisotropy observations critical for global analyses of seismic anisotropy. We envision a data system that would include a publicly available, next-generation, automated, searchable database capable of delivering the complete metadata associated with a given study. To this end, the data system would deliver the actual seismic waveform data used in published studies, the computer codes and processing criteria used to obtain the results, and tables and user-configurable maps of results from these studies. The goal of this approach would be to empower the user to reproduce published measurements, add new measurements using the same (or different) data selection criteria and codes, and/or build upon these results in new ways that require various parts of these metadata. This data system would provide essential information to scientists who use seismic anisotropy constraints in other data analyses and modeling efforts. It would provide a revolutionary new level of user access with the ability to reproduce all results included in the database, and would facilitate more rapid breakthroughs in new methods of imaging seismic anisotropy.

Author's personal copy

6. Concluding remarks

In this review paper, we have shown that knowledge of seismic anisotropy is fundamental for understanding the deformational processes involved in the evolution of continental regions. Several data analysis techniques exist that can help constrain seismic anisotropy; however, each technique used alone can generally determine only a portion of the anisotropic structure of a region. Analyses to date demonstrate that seismic anisotropy is almost always found in the crust but only contributes a small fraction of the total anisotropic signal recorded at the surface; therefore most of the anisotropy resides below the crust but its exact source and location are still under debate. Some workers suggest that lithospheric fabric is the primary cause of observed seismic anisotropy, while other workers suggest that the seismic anisotropy signal originates from sublithospheric structure.

Taking a comprehensive view of all current methods and results to date, we conclude that lithospheric and sublithospheric fabrics likely coexist in stable continental regions, with the predominance of one or the other depending on, among other things, a combination of local geologic complexity and regional plate motion velocity. The complexity of anisotropic structure in many regions precludes detection by all analysis methods. Further work involving the integration of complementary seismic datasets and additional geophysical data is therefore required to constrain the extent of seismic anisotropy present in each of these domains, and how it relates to past and present tectonic processes.

Acknowledgments

This paper has benefited from extensive discussions with Thorsten Becker, Kris Walker, Steve Gao, and Paul Silver. We also thank Ed. Garnero for fruitful anisotropy discussions over the past several years. Reviews by Thorsten Becker, Martha Savage, Goetz Bökelmann, and David Eaton significantly improved the clarity of this work. Thanks to Alan Jones and David Eaton for inviting this contribution to this PEPI special section. Funding from National Science Foundation grants EAR-0126199 and EAR-0305564 (M.J.F.) and EAR-0409509 (S.R.) provided financial support related to this work.

References

Aki, K., Kaminuma, K., 1957. Phase velocity of Love waves in Japan, part 1 Love waves from the Aleutian shock of March. Bull. Earthquake Res. Inst. Univ. Tokyo 41, 243–259.

Ammon, C.J., Randall, G.E., Zandt, G., 1990. On the nonuniqueness of receiver function inversions. J. Geophys. Res. 95, 15303–15319.

Anderson, D.L., 1961. Elastic wave propagation in layered anisotropic media. J. Geophys. Res. 66, 2953–2963.

Ando, M., Ishikawa, Y., Wada, H., 1980. S-wave anisotropy in the upper mantle under a volcanic area in Japan. Nature 286, 43–46.

Ando, M., Ishikawa, Y., 1982. Observations of shear-wave velocity polarization anisotropy beneath Honshu Japan: two masses with different polarizations in the upper mantle. J. Phys. Earth 30 (2), 191–199.

Ansel, V., Nataf, H.-C., 1989. Anisotropy beneath 9 stations of the GEOSCOPE broadband network as deduced from shear-wave splitting. Geophys. Res. Lett. 16, 409–412.

Audet, P., Mareschal, J.-C., 2004. Anisotropy of the flexural response of the lithosphere in the Canadian Shield. Geophys. Res. Lett. 31, L20601, doi:10.1029/2004GL021080.

Babuška, V., Cara, M., 1991. Seismic anisotropy in the earth. Modern Approaches in Geophysics, vol. 10. Kluwer, Boston.

Babuška, V., Plomerová, J., Šilený, J., 1984. Spatial variations of P-residuals and deep-structure of the European lithosphere. Geophys. J. R. Astron. Soc. 79 (1), 363–383.

Bamford, D., 1977. Pn velocity anisotropy in a continental upper mantle. Geophys. J. R. Astron. Soc. 49, 29–48.

Bank, C.-G., Bostock, M.G., Ellis, R., Cassidy, J., 2000. A reconnaissance teleseismic study of the upper mantle and transition zone beneath the Archean Slave craton in NW Canada. Tectonophysics 319 (3), 151–166.

Bank, C.-G., Bostock, M.G., 2003. Linearized inverse scattering of teleseismic waves for anisotropic crust and upper mantle structure: 2. Numerical examples and applications to data from Canadian stations. J. Geophys. Res. 108 (B5), 2259, doi:10.1029/2002JB001951.

Barruol, G., Silver, P.G., Vauchez, A., 1997. Seismic anisotropy in the eastern United States: deep structure of a complex continental plate. J. Geophys. Res. 102 (4), 8329–8348.

Barruol, G., Ben-Ismaïl, W., 2001. Upper mantle anisotropy beneath the African IRIS and GEOSCOPE stations. Geophys. J. Int. 146 (2), 549–561.

Becker, T.W., Kellogg, J.B., Ekström, G., O'Connell, R.J., 2003. Comparison of azimuthal seismic anisotropy from surface waves and finite strain from global mantle-circulation models. Geophys. J. Int. 155 (2), 696–714.

Becker, T.W., Chevrot, S., Schulte-Pelkum, V., Blackman, D.K., 2006a. Statistical properties of seismic anisotropy predicted by upper mantle geodynamic models. J. Geophys. Res., in press.

Becker, T.W., Schulte-Pelkum, V., Blackman, D.K., Kellogg, J.B., O'Connell, R.J., 2006b. Mantle flow under the western United States from shear wave splitting: no decoupling required, Earth Planet. Sci. Lett., in press.

Beghein, C., Trampert, J., 2003. Robust normal mode constraints on inner-core anisotropy from model space search. Science 299 (5606), 552–555.

Beghein, C., Trampert, J., 2004a. Probability density functions for radial anisotropy from fundamental mode surface wave data and the neighbourhood algorithm. Geophys. J. Int. 157 (3), 1163–1174.

Beghein, C., Trampert, J., 2004b. Probability density functions for radial anisotropy: implications for the upper 1200 km of the mantle. Earth Planet. Sci. Lett. 217 (1–2), 151–162.

Behn, M.D., Conrad, C.P., Silver, P.G., 2004. Detection of upper mantle flow associated with the African Superplume. Earth Planet. Sci. Lett. 224 (3–4), 259–274.

Author's personal copy

Ben-Ismaïl, W., Mainprice, D., 1998. An olivine fabric database: an overview of upper mantle fabrics and seismic anisotropy. Tectonophysics 296 (1–2), 145–157.

Ben-Ismaïl, W., Barruol, G., Mainprice, D., 2001. The Kaapvaal craton seismic anisotropy: petrophysical analyses of upper mantle kimberlite nodules. Geophys. Res. Lett. 28 (13), 2497–2500.

Blackman, D.K., et al., 1996. Teleseismic imaging of subaxial flow at mid-ocean ridges: traveltime effects of anisotropic mineral texture in the mantle. Geophys. J. Int. 127, 415–426.

Bleeker, W., Ketchum, L., Jackson, V., Villeneuve, M., 1999. The central Slave basement complex, part I: its structural topology and autochthonous cover. Can. J. Earth Sci. 36, 1083–1109.

Bökelmann, G.H.R., 1995. P-wave array polarization analysis and effective anisotropy of the brittle crust. Geophys. J. Int. 120, 145–162.

Bökelmann, G.H.R., 2002. Convection-driven motion of the North American craton: evidence from P-wave anisotropy. Geophys. J. Int. 148, 278–287.

Bormann, P., Grunthal, G., Kind, R., Montag, H., 1996. Upper mantle anisotropy beneath central Europe from SKS wave splitting: effects of absolute plate motion and lithosphere–asthenosphere boundary topography? J. Geodyn. 22 (1–2), 11–32.

Boschi, L., Ekström, G., 2002. New images of the Earth's upper mantle from measurements of surface wave phase velocity anomalies. J. Geophys. Res. 107 (B4), 1–20.

Bostock, M.G., Cassidy, J.F., 1995. Variations in SKS splitting across western Canada. Geophys. Res. Lett. 22 (1), 5–8.

Bostock, M.G., 1997. Anisotropic upper-mantle stratigraphy and architecture of the Slave craton. Nature 390, 392–395.

Bostock, M.G., 1998. Mantle stratigraphy and evolution of the Slave province. J. Geophys. Res. 103 (B9), 21183–21200.

Bostock, M.G., Rondenay, S., Shragge, J., 2001. Mulitiparameter two-dimensional inversion of scattered teleseismic body waves. 1. Theory for oblique incidence. J. Geophys. Res. 106 (12), 30771–30782.

Bostock, M.G., 2003. Linearized inverse scattering of teleseismic waves for anisotropic crust and mantle structure: 1. Theory. J. Geophys. Res. 108 (B5), 2258, doi:10.1029/2002JB001950.

Bowman, J.R., Ando, M., 1987. Shear-wave splitting in the upper-mantle wedge above the Tonga subduction zone. Geophys. J. R. Astron. Soc. 88, 25–41.

Bowring, S.A., Grotzinger, J.P., 1992. Implications of new chronostratigraphy for tectonic evolution of Wopmay orogen Northwestern Canadian Shield. Am. J. Sci. 292, 1–20.

Braun, M.G., Hirth, G., Parmentier, E.M., 2000. The effects of deep damp melting on mantle flow and melt generation beneath mid-ocean ridges. Earth Planet. Sci. Lett. 176 (3–4), 339–356.

Buchbinder, G.G.R., 1989. Azimuthal variations in P-wave travel times and shear-wave splitting in the Charlevoix seismic zone. Tectonophysics 165 (1–4), 293–302.

Cahen, L., Snelling, N.J., Delhal, J., Vail, J.R., 1984. The Geochronology and Evolution of Africa. Oxford University Press, NY, 512 pp.

Carlson, R.W., Grove, T.L., de Wit, M.J., Gurney, J.J., 1996. Anatomy of an Archean craton: a program for interdisciplinary studies of the Kaapvaal craton, southern Africa. Eos Trans. AGU 77, 273–277.

Carlson, R.W., et al., 2000. Continental growth, preservation and modification in southern Africa. GSA Today 20 (2), 1–7.

Chen, C.-W., Rondenay, S., Weeraratne, D.S., Yang, Y., Snyder, D.B., 2005. Upper mantle anisotropy and shear wave velocity structure beneath the Slave craton inferred from Rayleigh waves. Eos Trans. AGU 86 (52) (Fall Meeting Supplement, Abstract T22B-04, 2005).

Chen, W.P., Brudzinski, M.R., 2003. Seismic anisotropy in the mantle transition zone beneath Fiji-Tonga. Geophys. Res. Lett. 30 (13) (Art. No. 1682).

Chevrot, S., 2000. Multichannel analysis of shear wave splitting. J. Geophys. Res. 105 (B9), 21579–21590.

Chevrot, S., Favier, N., Komatitsch, D., 2004. Shear wave splitting in three-dimensional anisotropic media. Geophys. J. Int. 159 (2), 711–720.

Christoffel, E.B., 1877. Uber die Fortpflanzung von Stossen durch elastische feste Korper. Ann. Mater. 8, 193–243.

Clitheroe, G., van der Hilst, R.D., 1998. Complex anisotropy in the Australian lithosphere from shear-wave splitting in broad-band SKS-records. In: Braun, J., Dooley, J.C., Goleby, B., van der Hilst, R.D., Klootwijk, C. (Eds.), Structure and Evolution of the Australian Continent. Geodyn. Ser., vol. 26. AGU, Washington, DC, pp. 73–78.

Clowes, R.M., 1997. Lithoprobe phase IV: multidisciplinary studies of the evolution of the continent—a progress report. Geosci. Can. 23, 109–123.

Cook, F.A., van der Velden, A.J., Hall, K.W., Roberts, B.J., 1999. Frozen subduction in Canada's northwest territories: lithoprobe deep lithospheric reflection profiling of the western Canadian Shield. Tectonics 18, 1–24.

Crampin, S., Chesnokov, E.M., Hipkin, R.A., 1984. Seismic anisotropy: the state of the art. First Break 2 (3), 9–18.

Couvy, H., et al., 2004. Shear deformation experiments of forsterite at 11GPa-1400 degrees C in the multianvil apparatus. Eur. J. Miner. 16 (6), 877–889.

Crampin, S., King, D., 1977. Evidence for anisotropy in the upper mantle beneath eurasia from generalized higher mode surface waves. Geophys. J. R. Astron. Soc. 49, 59–85.

Davis, P.M., 2003. Azimuthal variation in seismic anisotropy of the southern California uppermost mantle. J. Geophys. Res. Solid Earth 108 (B1) (Art. No. 2052).

de Wit, M.J., et al., 1992. Formation of an Archaean continent. Nature 357 (6379), 553–562.

de Wit, M.J., Hart, R.A., 1993. Earth's earliest continental lithosphere, hydrothermal flux and crustal recycling. Lithos 30 (3–4), 309–335.

Debayle, E., 1999. SV-wave azimuthal anisotropy in the Australian upper mantle: preliminary results from automated Rayleigh waveform inversion. Geophys. J. Int. 137 (June (3)), 747–754.

Debayle, E., Kennett, B.L.N., 2000a. Anisotropy in the Australasian upper mantle from Love and Rayleigh waveform inversion. Earth Planet. Sci. Lett. 184, 339–351.

Debayle, E., Kennett, B.L.N., 2000b. The Australian continental upper mantle: structure and deformation inferred from surface waves. J. Geophys. Res. 105 (11), 25423–25450.

Debayle, E., Kennett, B., Priestley, K., 2005. Global azimuthal seismic anisotropy and the unique plate-motion deformation of Australia. Nature 433 (7025), 509–512.

Dueker, K.G., Sheehan, A.F., 1997. Mantle discontinuity structure from midpoint stacks of converted p to s waves across the Yellowstone hotspot track. J. Geophys. Res. 102, 8313–8327.

Dziewonski, A.M., Anderson, D.L., 1981. Preliminary reference earth model. Phys. Earth Planet. Int. 25, 297–356.

Eaton, D., Frederiksen, A., Miong, S.-Y., 2004a. Shear-wave splitting observations in the lower Great Lakes region: evidence for regional anisotropic domains and keel-modified asthenospheric flow. Geophys. Res. Lett. 31, L07610, doi:10.1029/2004GL019438.

Eaton, D.W., Jones, A.G., Ferguson, I.J., 2004b. Lithospheric anisotropy structure inferred from collocated teleseismic and magnetotelluric observations: Great Slave Lake shear zone,

Author's personal copy

northern Canada. Geophys. Res. Lett. 31, L19614, doi:10.1029/2004GL020939.

Eberhart-Phillips, D., Henderson, C.M., 2004. Including anisotropy in 3-D velocity inversion and application to Marlborough, New Zealand. Geophys. J. Int. 156 (2), 237–254.

Ekström, G., 2001. Mapping azimuthal anisotropy of intermediate-period surface waves. EOS Trans. AGU 82 (47), S51E-06 (Abstract).

Favier, N., Chevrot, S., 2003. Sensitivity kernels for shear wave splitting in transverse isotropic media. Geophys. J. Int. 153 (1), 213–228.

Fischer, K.M., Parmentier, E.M., Stine, A.R., Wolf, E.R., 2000. Modeling anisotropy and plate-driven flow in the Tonga subduction zone back arc. J. Geophys. Res. 105 (B7), 16181–16191.

Fischer, K.M., Forsyth, D.W., Li, A., Hung, S.H., 2005. Imaging three-dimensional anisotropy with broadband arrays. In: Levander, A., Nolet, G. (Eds.), SeismicEarth: Array Analysis of Broadband Seismograms. Geophysical Monograph 157, AGU, pp. 99–116.

Forsyth, D.W., 1975. The early structural evolution and anisotropy of the oceanic upper mantle. Geophys. J. R. Astron. Soc. 43, 103–162.

Forsyth, D.W., Li, A., 2005. Array analysis of two-dimensional variations of surface wave phase velocity and azimuthal anisotropy in the presence of multipathing interference. In: Levander, A., Nolet, G. (Eds.), Seismic Data Analysis and Imaging with Global and Local Arrays. AGU, Washington, DC.

Fouch, M.J., Fischer, K.M., 1996. Mantle anisotropy beneath northwest Pacific subduction zones. J. Geophys. Res. 101 (B7), 15987–16002.

Fouch, M.J., Fischer, K.M., 1998. Shear wave anisotropy in the Mariana subduction zone. Geophys. Res. Lett. 25 (8), 1221–1224.

Fouch, M.J., Fischer, K.M., Parmentier, E.M., Wysession, M.E., Clarke, T.J., 2000. Shear wave splitting, continental keels, and patterns of mantle flow. J. Geophys. Res. 105 (B3), 6255–6275.

Fouch, M.J., James, D.E., VanDecar, J.C., van der Lee, S., The Kaapvaal Seismic Group, 2004a. Mantle seismic structure beneath the Kaapvaal and Zimbabwe cratons. S. Afr. J. Geol. 107 (1–2), 35–46.

Fouch, M.J., Silver, P.G., Bell, D.R., Lee, J.N., 2004b. Small-scale variations in seismic anisotropy beneath Kimberley, South Africa. Geophys. J. Int. 157 (2), 764–774.

Frederiksen, A.W., Bostock, M.G., 2000. Modelling teleseismic waves in dipping anisotropic structures. Geophys. J. Int. 141, 401–412.

Frederiksen, A.W., Folsom, H., Zandt, G., 2003. Neighbourhood inversion of teleseismic Ps conversions for anisotropy and layer dip. Geophys. J. Int. 155, 200–212.

Freybourger, M., Gaherty, J.B., Jordan, T.H., The Kaapvaal Seismic Group, 2001. Structure of the Kaapvaal craton from surface waves. Geophys. Res. Lett. 28 (13), 2489–2492.

Gaherty, J.B., Kato, M., Jordan, T.H., 1999. Seismological structure of the upper mantle: a regional comparison of seismic layering. Phys. Earth Planet. Int. 110, 21–41.

Gaherty, J.B., Jordan, T.H., 1995. Lehmann discontinuity as the base of an anisotropic layer beneath continents. Science 268 (5216), 1468–1471.

Gaherty, J.B., 2001. Seismic evidence for hotspot-induced buoyant flow beneath the Reykjanes Ridge. Science 293 (5535), 1645–1647.

Gaherty, J.B., 2004. A surface wave analysis of seismic anisotropy beneath eastern North America. Geophys. J. Int. 158 (3), 1053–1066.

Gao, S., et al., 1997. SKS splitting beneath continental rift zones. J. Geophys. Res. 102 (B10), 22781–22797.

Garnero, E.J., 2000. Heterogeneity of the lowermost mantle. Ann. Rev. Earth Planet. Sci. 28, 509–537.

Gee, L.S., Jordan, T.H., 1992. Generalized seismological data functionals. Geophys. J. Int. 111, 363–390.

Girardin, N., Farra, V., 1998. Azimuthal anisotropy in the upper mantle from observations of P-to-S converted phases: application to southeast Australia. Geophys. J. Int. 133, 615–629.

Gledhill, K.R., 1993. Shear waves recorded on close-spaced seismographs: I. Shear-wave splitting results. Can. J. Expl. Geophys. 29 (1), 285–298.

Gledhill, K., Gubbins, D., 1996. SKS splitting and the seismic anisotropy of the mantle beneath the Hikurangi subduction zone, New Zealand. Phys. Earth Planet. Int. 95 (3–4), 227–236.

Gripp, A.E., Gordon, R.G., 1990. Current plate velocities relative to the hotspots incorporating the Nuvel-1 global plate motion model. Geophys. Res. Lett. 17 (8), 1109–1112.

Gripp, A.E., Gordon, R.G., 2002. Young tracks of hotspots and current plate velocities. Geophys. J. Int. 150 (2), 321–361.

Guilbert, J., Poupinet, G., Jiang, M., 1996. A study of azimuthal P residuals and shear-wave splitting across the Kunlun range (Northern Tibetan plateau). Phys. Earth Planet. Int. 95 (3–4), 167–174.

Gung, Y.C., Panning, M., Romanowicz, B., 2003. Global anisotropy and the thickness of continents. Nature 422 (6933), 707–711.

Hall, C.E., Fischer, K.M., Parmentier, E.M., Blackman, D.K., 2000. The influence of plate motions on three-dimensional back arc mantle flow and shear wave splitting. J. Geophys. Res. 105 (B12), 28009–28033.

Hartog, R., Schwartz, S.Y., 2000. Subduction-induced strain in the upper mantle east of the Mendocino triple junction, California. J. Geophys. Res. 105 (B4), 7909–7930.

Hearn, T.M., 1996. Anisotropic Pn tomography in the Western United States. J. Geophys. Res. 101 (B4), 8403–8414.

Hedlin, M.A.H., Shearer, P.M., 2000. An analysis of large-scale variations in small-scale mantle heterogeneity using global seismographic network recordings of precursors to PKP. J. Geophys. Res. 105 (B6), 13655–13673.

Heintz, M., Kennett, B.L.N., 2005. Continental scale shear wave splitting analysis: investigation of seismic anisotropy underneath the Australian continent. Earth Planet. Sci. Lett. 236, 106–119.

Helbig, K., Szaraniec, E., 2000. The historical roots of seismic anisotropy. In: Ikelle, L., Gangi, A. (Eds.), Anisotropy 2000: Fractures, Converted Waves and Case Studies. SEG, Tulsa, OK, pp. 1–11.

Hess, H.H., 1964. Seismic anisotropy of the uppermost mantle under oceans. Nature 203 (4945), 629–631.

Hirn, A., 1977. Anisotropy in continental upper mantle—possible evidence from explosion seismology. Geophys. J. R. Astron. Soc. 49 (1), 49–58.

Hoffman, P.F., 1989. Precambrian geology and tectonic history of North America. In: Bally, W.W., Palmer, A.R. (Eds.), The Geology of North America—An Overview. Geol. Soc. Am., Boulder, CO, pp. 447–512.

Hoffman, P.F., 1990. Geological constraints on the origin of the mantle root beneath the Canadian shield. Philos. Trans. R. Soc. Lond. Ser. A 331, 523–532.

Holtzman, B.K., et al., 2003. Melt segregation and strain partitioning: implications for seismic anisotropy and mantle flow. Science 301 (5637), 1227–1230.

Iidaka, T., Niu, F., 1998. Evidence for an anisotropic lower mantle beneath eastern Asia: comparison of shear-wave splitting data of SKS and P660s. Geophys. Res. Lett. 25 (5), 675–678.

Author's personal copy

Ishii, M., Dziewonski, A.M., 2003. Distinct seismic anisotropy at the centre of the Earth. Phys. Earth Planet. Int. 140 (1–3), 203–217.

James, D.E., Assumpçao, M., 1996. Tectonic implications of S-wave anisotropy beneath SE Brazil. Geophys. J. Int. 126, 1–10.

James, D.E., Fouch, M.J., VanDecar, J.C., van der Lee, S., The Kaapvaal Seismic Group, 2001. Tectospheric structure beneath southern Africa. Geophys. Res. Lett. 28 (13), 2485–2488.

Ji, S., Zhao, X., Francis, D., 1994. Calibration of shear-wave splitting in the subcontinental upper mantle beneath active orogenic belts using ultramafic xenoliths from the Canadian Cordillera and Alaska. Tectonophysics 239 (1–4), 1–27.

Ji, S., Rondenay, S., Mareschal, M., Sénéchal, G., 1996. Obliquity between seismic and electrical anisotropies as a potential indicator of movement sense for ductile shear zones in the upper mantle. Geology 24 (11), 1033–1036.

Jung, H., Karato, S., 2001. Water-induced fabric transitions in olivine. Science 293 (5534), 1460–1463.

Kaminski, E., Ribe, N.M., 2001. A kinematic model for recrystallization and texture development in olivine polycrystals. Earth Planet. Sci. Lett. 189 (3–4), 253–267.

Kamo, S.L., Krogh, T.E., Kumarapeli, P.S., 1995. Age of the Grenville dyke swarm, Ontario-Quebec: implications for the timing of Iapetan rifting. Can. J. Earth Sci. 32, 273–280.

Karato, S., 1987. Seismic anisotropy due to lattice preferred orientation of minerals: kinematic or dynamic? In: Manghnani, M.H., Syono, S. (Eds.), High-Pressure Research in Mineral Physics. Geophysical Monograph Ser. AGU, Washington, DC, pp. 455–471.

Karato, S.I., Wu, P., 1993. Rheology of the upper mantle: a synthesis. Science 260 (5109), 771–778.

Karato, S., Jung, H., 1998. Water, partial melting and the origin of the seismic low velocity and high attenuation zone in the upper mantle. Earth Planet. Sci. Lett. 157 (3–4), 193–207.

Kato, M., Jordan, T.H., 1999. Seismic structure of the upper mantle beneath the western Philippine Sea. Phys. Earth Planet. Int. 110 (3–4), 263–283.

Katayama, I., Jung, H., Karato, S., 2004. New type of olivine fabric from deformation experiments at modest water content and low stress. Geology 32 (12), 1045–1048.

Katayama, I., Karato, S., Brandon, M., 2005. Evidence of high water content in the deep upper mantle inferred from deformation microstructures. Geology 33 (7), 613–616.

Katzman, R., Zhao, L., Jordan, T.H., 1998. High-resolution, two-dimensional vertical tomography of the central Pacific mantle using ScS reverberations and frequency-dependent travel times. J. Geophys. Res. 103 (B8), 17933–17971.

Kawasaki, I., Kon, N.F., 1984. Azimuthal anisotropy of surface waves and the possible type of the seismic anisotropy due to preferred orientation of olivine in the uppermost mantle beneath the Pacific Ocean. J. Phys. Earth 32 (3), 229–244.

Kay, I., et al., 1999a. Shear wave splitting observations in the Archean craton of western Superior. Geophys. Res. Lett. 26 (17), 2669–2672.

Kay, I., Sol, S., Kendall, J.-M., Thomson, C., White, D., Asudeh, I., Roberts, B., Francis, D., 1999b. Shear wave splitting observations in the Archean craton of Western Superior. Geophys. Res. Lett. 26 (17), 2669–2672.

Keith, C.M., Crampin, S., 1977. Seismic body waves in anisotropic media: reflection and refraction at a plane interface. Geophys. J. R. Astron. Soc. 49 (1), 181–208.

Kellett, R.L., Barnes, A.E., Rive, M., 1994. The deep structure of the Grenville Front: a new perspective from western Quebec. Can. J. Earth Sci. 31, 282–292.

Kendall, J.M., 1994. Teleseismic arrivals at a mid-ocean ridge: effects of mantle melt and anisotropy. Geophys. Res. Lett. 21 (4), 301–304.

Kendall, J.M., 2000. Seismic anisotropy in boundary layers of the mantle. In: Karato, S.I., Forte, A.M., Liebermann, R.C., Masters, G., Stixrude, L. (Eds.), Earth's Deep Interior: Mineral Physics and Tomography from the Atomic to the Global Scale. Geophysical Monograph AGU, Washington, DC, United States, pp. 133–159.

Kern, H., 1993. P- and S-wave anisotropy and shear-wave splitting at pressure and temperature in possible mantle rocks and their relation to the rock fabric. Phys. Earth Planet. Int. 78 (3–4), 245–256.

Kern, H., Burlini, L., Ashchepkov, I.V., 1996. Fabric-related seismic anisotropy in upper-mantle xenoliths: evidence from measurements and calculations. Phys. Earth Planet. Int. 95 (3–4), 195–209.

Kind, R., Kosarev, G.L., Makeyeva, L.I., Vinnik, L.P., 1985. Observations of laterally inhomogeneous anisotropy in the continental lithosphere. Nature 318 (6044), 358–361.

Klitgord, K.D., Hutchinson, D.R., Schouten, H., 1988. U.S. Atlantic continental margin: structural and tectonic framework. In: Sheridan, R.E., Grow, J.A. (Eds.), The Atlantic Continental Margin. U.S. Geol. Soc. Am., Boulder, CO, pp. 19–51.

Laske, G., Masters, G., 1998. Surface-wave polarization data and global anisotropic structure. Geophys. J. Int. 132 (3), 508–520.

Lassak, T.M., Fouch, M.J., Hall, C.E., Kaminski, E., 2006. Seismic characterization of mantle flow in subduction systems: can we resolve a hydrated mantle wedge? Earth Planet. Sci. Lett. 243, 632–649.

Lay, T., Williams, Q., Garnero, E.J., Kellogg, L., Wysession, M.E., 1998. Seismic wave anisotropy in the D" region and its implications. In: Gurnis, M., Wysession, M.E., Knittle, E., Buffett, B.A. (Eds.), The Core–Mantle Boundary Region. AGU, Washington, DC, pp. 299–318.

Levin, V., Menke, W., Lerner-Lam, A., 1996. Seismic anisotropy in the north-eastern US as a source of significant teleseismic P traveltime anomalies. Geophys. J. Int. 126, 593–603.

Levin, V., Park, J., 1997. P-SH conversions in a flat-layered medium with anisotropy of arbitrary orientation. Geophys. J. Int. 131, 153–166.

Levin, V., Menke, W., Park, J., 1999. Shear wave splitting in the Appalachians and the Urals: a case for multilayered anisotropy. J. Geophys. Res. 104 (B8), 17975–17993.

Li, A., Forsyth, D.W., Fisher, K.M., 2003. Shear velocity structure and azimuthal anisotropy beneath eastern North America from Rayleigh wave inversion. J. Geophys. Res. 108 (B8) (Art. No. 2362).

Long, C., Christensen, N.I., 2000. Seismic anisotropy of South African upper mantle xenoliths. Earth Planet. Sci. Lett. 179 (3–4), 551–565.

Mainprice, D., Nicolas, A., 1989. Development of shape and lattice preferred orientations: application to the seismic anisotropy of the lower crust. J. Struct. Geol. 11 (1–2), 175–189.

Mainprice, D., Silver, P.G., 1993. Interpretation of SKS-waves using samples from the subcontinental lithosphere. Phys. Earth Planet. Int. 78 (3–4), 257–280.

Mainprice, D., Tommasi, A., Couvy, H., Cordier, P., Frost, D.J., 2005. Pressure sensitivity of olivine slip systems and seismic anisotropy of Earth's upper mantle. Nature 433 (7027), 731–733.

Mareschal, M., Kellett, R.L., Kurtz, R.D., Ludden, J.N., Ji, S., Bailey, R.C., 1995. Archaean cratonic roots, mantle shear zones and deep electrical anisotropy. Nature 375 (May), 134–137.

Marson-Pidgeon, K., Savage, M.K., 1997. Frequency-dependent anisotropy in the Wellington region New Zealand. Geophys. Res. Lett. 24 (24), 3297–3300.

Authors personal copy

McKenzie, D., 1979. Finite deformation during fluid flow. Geophys. J. R. Astron. Soc. 58, 687–715.

Mehl, L., Hacker, B.R., Hirth, G., Kelemen, P.B., 2003. Arc-parallel flow within the mantle wedge: evidence from the accreted Talkeetna arc, south central Alaska. J. Geophys. Res. Solid Earth 108. (B8).

Meissner, R., Mooney, W.D., Artemieva, I., 2002. Seismic anisotropy and mantle creep in young orogens. Geophys. J. Int. 149 (1), 1–14.

Menke, W., Levin, V., 2003. The cross-convolution method for interpreting SKS splitting observations, with application to one and two-layer anisotropic earth models. Geophys. J. Int. 154 (2), 379–392.

Montagner, J.P., Nataf, H.C., 1986. A simple method for inverting the azimuthal anisotropy of surface waves. J. Geophys. Res. 91, 511–520.

Montagner, J.P., Kennett, B.L.N., 1996. How to reconcile body-wave and normal-mode reference earth models. Geophys. J. Int. 125 (1), 229–248.

Montagner, J.-P., Guillot, L., 2000. Seismic anisotropy in the Earth's mantle. In: Boschi, E., Ekström, G., Morelli, A. (Eds.), Problems in Geophysics for the New Millenium. Istituto Nazionale di Geofisica e Vulcanologia, Editrice Compositori, Bologna, Italy, pp. 217–253.

Montagner, J.P., Griot-Pommera, D.A., Lave, J., 2000. How to relate body wave and surface wave anisotropy? J. Geophys. Res. 105 (B8), 19015–19027.

Montagner, J.P., 2002. Seismic anisotropy tomography. Imag. Complex Media Acoustic Seismic Waves 84, 191–231.

Musacchio, G., White, D.J., Asudeh, I., Thomson, C.J., 2004. Lithospheric structure and composition of the Archean western Superior Province from seismic refraction/wide-angle reflection and gravity modeling. J. Geophys. Res. 109 (B3), B03304, doi:10.1029/2003JB002427.

Nicolas, A., Christensen, N.I., 1987. Formation of anisotropy in upper mantle peridotites: a review. In: Fuchs, K., Froidevaux, C. (Eds.), Composition, Structure, and Dynamics of the Lithosphere–Asthenosphere System. Geodyn. Ser. AGU, Washington, DC, pp. 111–123.

Niu, F., Perez, A.M., 2004. Seismic anisotropy in the lower mantle: a comparison of waveform splitting of SKS and SKKS. Geophys. Res. Lett. 31 (24), L24612.

Nolet, G., 1990. Partitioned waveform inversion and two-dimensional structure under the network of autonomously recording seismographs. J. Geophys. Res. 95, 8499–8512.

Nyblade, A.A., Birt, C., Langston, C.A., Owens, T.J., Last, R.J., 1996. Seismic experiment reveals rifting of craton in Tanzania. Eos Trans. AGU 77, 517.

Nyblade, A.A., Owens, T.J., Gurrola, H., Ritsema, J., Langston, C.A., 2000. Seismic evidence for a deep upper mantle thermal anomaly beneath east Africa. Geology 28, 599–602.

Oda, H., 2005. An attempt to estimate isotropic and anisotropic lateral structure of the earth by spectral inversion incorporating mixed coupling. Geophys. J. Int. 160 (2), 667–682.

Özalaybey, S., Savage, M.K., 1995. Shear-wave splitting beneath western United States in relation to plate tectonics. J. Geophys. Res. 100 (B9), 18135–18149.

Özalaybey, S., Chen, W.P., 1999. Frequency-dependent analysis of SKS/SKKS waveforms observed in Australia: evidence for null birefringence. Phys. Earth Planet. Int. 114 (July (3–4)), 197–210.

Park, J., Levin, V., 2002. Seismic anisotropy: tracing plate dynamics in the mantle. Science 296 (5567), 485–489.

Park, J., Yuan, H., Levin, V., 2004. Subduction zone anisotropy beneath Corvallis Oregon: a serpentinite skid mark of trench-parallel terrane migration? J. Geophys. Res. 109, B10306, doi:10.1029/2003JB002718.

Podolefsky, N.S., Zhong, S.J., McNamara, A.K., 2004. The anisotropic and rheological structure of the oceanic upper mantle from a simple model of plate shear. Geophys. J. Int. 158 (1), 287–296.

Qiu, X., Priestley, K., McKenzie, D., 1996. Average lithospheric structure of southern Africa. Geophys. J. Int. 127, 563–587.

Raitt, R., Shor, G., Francis, T., Morris, G., 1969. Anisotropy of the pacific upper mantle. J. Geophys. Res. 74, 3095–3109.

Ribe, N.M., 1989. Seismic anisotropy and mantle flow. J. Geophys. Res. 94, 4213–4223.

Ribe, N.M., Yu, Y., 1991. A theory for plastic deformation and textural evolution of olivine polycrystals. J. Geophys. Res. 96 (B5), 8325–8355.

Ribe, N.M., 1992. On the relation between seismic anisotropy and finite strain. J. Geophys. Res. 97, 8737–8747.

Ritsema, J., van Heijst, H., 2000. A new seismic model of the upper mantle beneath Africa. Geology 28, 63–66.

Rivers, T., Martignole, J., Gower, C.F., Davidson, A., 1989. New tectonic divisions of the Grenville province, southeast Canadian Shield. Tectonics 8 (1), 63–84.

Rivers, T., 1997. Lithotectonic elements of the Grenville province: review and tectonic implications. Precambrian Res. 86, 117–154.

Rondenay, S., et al., 2000. Teleseismic studies of the lithoshpere below the Abitibi-Grenville Lithoprobe transect. Can. J. Earth Sci. 37, 415–426.

Rondenay, S., Bostock, M.G., Hearn, T.M., White, D.J., Ellis, R.M., 2000a. Lithospheric assembly and modification of the SE Canadian Shield: Abitibi-Grenville teleseismic experiment. J. Geophys. Res. 105 (B6), 13735–13754.

Rondenay, S., Bostock, M.G., Hearn, T.M., White, D.J., Wu, H., Sénéchal, G., Ji, S., Mareschal, M., 2000b. Teleseismic studies of the lithosphere below the Abitibi-Grenville Lithoprobe transect. Can. J. Earth Sci. 37, 415–426.

Rondenay, S., Bostock, M.G., Shragge, J., 2001. Multiparameter two-dimensional inversion of scattered teleseismic body waves 3 Application to the Cascadia 1993 data set. J. Geophys. Res. 106 (12), 30795–30807.

Rondenay, S., Fouch, M.J. Discontinuity structure beneath Kimberley, South Africa, in preparation.

Rost, S., Thomas, C., 2002. Array seismology: methods and applications. Rev. Geophys. 40 (3) (Art. No. 1008).

Rudzki, M.P., 1897. Über die Gestalt elastischer Wellen in Gesteinen II Studie aus der Theorie der Erdbebenwellen. Bull. Acad. Sci. Cracow, 387–393.

Rümpker, G., Ryberg, T., 2000. New "Fresnel-zone" estimates for shear-wave splitting observations from finite-difference modeling. Geophys. Res. Lett. 27 (13), 2005–2008.

Saltzer, R.L., 2002. Upper mantle structure of the Kaapvaal craton from surface wave analysis—a second look. Geophys. Res. Lett. 29 (6), 1–4, 17.

Sambridge, M., 1999a. Geophysical inversion with a neighbourhood algorithm—I. Searching a parameter space. Geophys. J. Int. 138 (2), 479–494.

Sambridge, M., 1999b. Geophysical inversion with a neighbourhood algorithm—II. Appraising the ensemble. Geophys. J. Int. 138 (3), 727–746.

Savage, M.K., Silver, P.G., Meyer, R.P., 1990. Observations of teleseismic shear-wave splitting in the Basin and Range from portable and permanent stations. Geophys. Res. Lett. 17 (1), 21–24.

Authors personal copy

Savage, M.K., Silver, P.G., 1993. Mantle deformation and tectonics: constraints from seismic anisotropy in the western United-States. Phys. Earth Planet. Int. 78 (3–4), 207–227.

Savage, M.K., 1998. Lower crustal anisotropy or dipping boundaries? Effects on receiver functions and a case study in New Zealand. J. Geophys. Res. 103, 15069–15087.

Savage, M.K., 1999. Seismic anisotropy and mantle deformation: what have we learned from shear wave splitting? Rev. Geophys. 37 (1), 65–106.

Schmid, C., Goes, S., van der Lee, S., Giardini, D., 2002. Fate of the Cenozoic Farallon slab from a comparison of kinematic thermal modeling with tomographic images. Earth Planet. Sci. Lett. 204 (1–2), 17–32.

Schulte-Pelkum, V., Blackman, D.K., 2003. A synthesis of seismic P and S anisotropy. Geophys. J. Int. 154 (1), 166–178.

Schulte-Pelkum, V., Masters, G., Shearer, P.M., 2001. Upper mantle anistropy from long-period P polarization. J. Geophys. Res. 106 (B10), 21917–21934.

Sénéchal, G., Rondenay, S., Mareschal, M., Guilbert, J., Poupinet, G., 1996. Seismic and electrical anisotropies in the lithosphere across the Grenville Front. Geophys. Res. Lett. 23, 2255–2258.

Shapiro, N.M., Ritzwoller, M.H., 2002. Monte-Carlo inversion for a global shear velocity model of the crust and upper mantle. Geophys. J. Int. 151 (1), 88–105.

Shaw, R.D., Wellman, P., Gunn, P.J., Whitaker, A.J., Tarlowski, C., Morse, M.P., 1996. Guide to using the Australian Crustal Elements Map. Australian Geological Survey Organisation, Record 1996/30.

Silver, P.G., Chan, W.W., 1988. Implications for continental structure and evolution from seismic anisotropy. Nature 335 (6185), 34–39.

Silver, P.G., Chan, W.W., 1991. Shear wave splitting and subcontinental mantle deformation. J. Geophys. Res. 96 (B10), 16429–16454.

Silver, P.G., Kaneshima, S., 1993. Constraints on mantle anisotropy beneath Precambrian North America from a transportable teleseismic experiment. Geophys. Res. Lett. 20 (12), 1127–1130.

Silver, P.G., 1996. Seismic anisotropy beneath the continents: probing the depths of geology. Ann. Rev. Earth Planet. Sci. 24, 385–432.

Silver, P.G., Gao, S.S., Liu, K.H., The Kaapvaal Seismic Group, 2001. Mantle deformation beneath southern Africa. Geophys. Res. Lett. 28 (13), 2493–2496.

Silver, P.G., Fouch, M.J., Gao, S.S., Schmitz, M., 2004. Seismic anisotropy, mantle fabric, and the magmatic evolution of Precambrian southern Africa. S. Afr. J. Geol. 107. (1–2).

Simons, F.J., van der Hilst, R.D., Montagner, J.-P., Zielhuis, A., 2002. Multimode Rayleigh wave inversion for heterogeneity and azimuthal anisotropy of the Australian upper mantle. Geophys. J. Int. 151 (3), 738–754.

Simons, F.J., van der Hilst, R.D., 2003. Seismic and mechanical anisotropy and the past and present deformation of the Australian lithosphere. Earth Planet. Sci. Lett. 211 (3–4), 271–286.

Simons, F.J., van der Hilst, R.D., Zuber, M.T., 2003. Spatio-spectral localization of isostatic coherence anisotropy in Australia and its relation to seismic anisotropy: implications for lithospheric deformation. J. Geophys. Res. 108 (B5), 2250, doi:10.1029/2001JB000704.

Simpson, F., 2002. Intensity and direction of lattice-preferred orientation of olivine: are electrical and seismic anisotropies of the Australian mantle reconcilable? Earth Planet. Sci. Lett. 203 (1), 535–547.

Smith, G.P., Ekström, G., 1999. A global study of Pn anisotropy beneath continents. J. Geophys. Res. 104 (B1), 963–980.

Smith, D.B., Ritzwoller, M.H., Shapiro, N.M., 2004. Stratification of anisotropy in the Pacific upper mantle. J. Geophys. Res. 109 (B11), B11309.

Snyder, D.B., Bostock, M.G., Lockhart, G.D., 2003. Two anisotropic layers in the Slave craton. Lithos 71, 529–539.

Snyder, D.B., Rondenay, S., Bostock, M.G., Lockhart, G.D., 2004. Mapping the mantle lithosphere for diamond potential. Lithos 77, 859–872.

Soedjatmiko, B., Christensen, N.I., 2000. Seismic anisotropy under extended crust: evidence from upper mantle xenoliths, Cima Volcanic Field, California. Tectonophysics 321 (3), 279–296.

Tanimoto, T., Anderson, D.L., 1985. Lateral heterogeneity and azimuthal anisotropy of the upper mantle: Love and Rayleigh waves 100–250 s. J. Geophys. Res. 90, 1842–1858.

Teanby, N.A., Kendall, J.M., Van der Baan, M., 2004. Automation of shear-wave splitting measurements using cluster analysis. Bull. Seismol. Soc. Am. 94 (2), 453–463.

Tommasi, A., 1998. Forward modeling of the development of seismic anisotropy in the upper mantle. Earth Planet. Sci. Lett. 160 (1–2), 1–13.

Tommasi, A., Mainprice, D., Cordier, P., Thoraval, C., Couvy, H., 2004a. Strain-induced seismic anisotropy of wadsleyite polycrystals and flow patterns in the mantle transition zone. J. Geophys. Res. 109 (B12).

Tommasi, A., Godard, M., Coromina, G., Dautria, J.-M., Barsczus, H., 2004b. Seismic anisotropy and compositionally induced velocity anomalies in the lithosphere above mantle plumes: a petrological and microstructural study of mantle xenoliths from French Polynesia. Earth Planet. Sci. Lett. 227 (3–4), 539–556.

Trampert, J., Woodhouse, J.H., 2001. Assessment of global phase velocity models. Geophys. J. Int. 144 (1), 165–174.

Trampert, J., van Heijst, H.J., 2002. Global azimuthal anisotropy in the transition zone. Science 296 (5571), 1297–1299.

Tromp, J., 1993. Support for anisotropy of the Earth's inner core from free oscillations. Nature 366, 678–681.

van der Hilst, R.D., Kennett, B.L.N., Christie, D., Grant, J., 1994. Project Skippy explores the lithosphere and mantle beneath Australia. Eos Trans. AGU 75, 177–181.

van der Lee, S., Nolet, G., 1997. Upper mantle S velocity structure of North America. J. Geophys. Res. 102 (B10), 22815–22838.

Vauchez, A., Dineur, F., Rudnick, R., 2005. Microstructure, texture and seismic anisotropy of the lithospheric mantle above a mantle plume: insights from the Labait volcano xenoliths (Tanzania). Earth Planet. Sci. Lett. 232 (3–4), 295–314.

Vinnik, L., 1977. Detection of waves converted from P to SV in the mantle. Phys. Earth Planet. Int. 15, 39–45.

Vinnik, L.P., Kosarev, G., Makeeva, L., 1984. Lithosphere anisotropy from the observation of SKS and SKKS waves. Doklady Akad. Nauk. USSR 278 (6), 1335–1339.

Vinnik, L.P., Farra, V., Romanowicz, B., 1989. Azimuthal anisotropy in the Earth from observations of SKS at GEOSCOPE and NARS broadband stations. Bull. Seismol. Soc. Am. 79 (5), 1542–1558.

Vinnik, L.P., Makeyeva, L.I., Milev, A., Usenko, A.Y., 1992. Global patterns of azimuthal anisotropy and deformations in the continental mantle. Geophys. J. Int. 111, 433–447.

Vinnik, L.P., Green, R.W.E., Nicolaysen, L.O., 1995. Recent deformations of the deep continental root beneath southern Africa. Nature 375, 50–52.

Author's personal copy

Vinnik, L.P., Green, R.W.E., Nicolaysen, L.O., 1996. Seismic constraints on dynamics of the mantle of the Kaapvaal craton. Phys. Earth Planet. Int. 95 (3–4), 139–151.

Vinnik, L., Kurnik, E., Farra, V., 2005. Lehmann discontinuity beneath North America: no role for seismic anisotropy. Geophys. Res. Lett. 32 (9).

Walker, K.T., Nyblade, A.A., Klemperer, S.L., Bökelmann, G.H.R., Owens, T.J., 2004. On the relationship between extension and anisotropy: constraints from shear-wave splitting across the East African Plateau. J. Geophys. Res. 109 (B8), B08302.

Weeraratne, D.S., Forsyth, D.W., Fischer, K.M., Nyblade, A.A., 2003. Evidence for an upper mantle plume beneath the Tanzanian craton from Rayleigh wave tomography. J. Geophys. Res. Solid Earth 108 (B9) (Art. No. 2427).

Wenk, H.-R., Bennett, K., Canova, G.R., Molinari, A., 1991. Modeling plastic deformation of peridotite with the self-consistent theory. J. Geophys. Res. 96 (B5), 8337–8349.

Wenk, H.R., Tomé, C.N., 1999. Modeling dynamic recrystallization of olivine aggregates deformed in simple shear. J. Geophys. Res. 104 (B11), 25513–25527.

Wolfe, C.J., Silver, P.G., 1998. Seismic anisotropy of oceanic upper mantle: shear wave splitting methodologies and observations. J. Geophys. Res. 103 (B1), 749–771.

Wookey, J., Kendall, J.M., Barruol, G., 2002. Mid-mantle deformation inferred from seismic anisotropy. Nature 415 (6873), 777–780.

Wookey, J., Kendall, J.M., 2004. Evidence of midmantle anisotropy from shear wave splitting and the influence of shear-coupled P-waves. J. Geophys. Res. 109 (B07), B07309.

Wysession, M.E., 1996. How well do we utilize global seismicity? Bull. Seismol. Soc. Am. 86 (5), 1207–1219.

Zhang, S., Karato, S., 1995. Lattice preferred orientation of olivine aggregates deformed in simple shear. Nature 375, 774–777.

Zhang, S.Q., Karato, S., Gerald, J.F., Faul, U.H., Zhou, Y., 2000. Simple shear deformation of olivine aggregates. Tectonophysics 316 (1–2), 133–152.

Zimmerman, M.E., Zhang, S.Q., Kohlstedt, D.L., Karato, S., 1999. Melt distribution in mantle rocks deformed in shear. Geophys. Res. Lett. 26 (10), 1505–1508.

Author's personal copy